JOURNAL OF GEOPHYSICAL RESEARCH, VOL. 106, NO. C4, PAGES 7107–7124, APRIL 15, 2001

Hydrography, nutrients, and carbon pools in the Pacific sector of the Southern Ocean: Implications for carbon flux

Kendra L. Daly,[1,2] Walker O. Smith, Jr.,[3] Gregory C. Johnson,[4]
Giacomo R. DiTullio,[5] David R. Jones[5,6] Calvin W. Mordy,[7]
Richard A. Feely,[4] Dennis A. Hansell,[8,9] and Jia-Zhong Zhang[10]

Abstract. We investigated the hydrography, nutrients, and dissolved and particulate carbon pools in the western Pacific sector of the Antarctic Circumpolar Current (ACC) during austral summer 1996 to assess the region's role in the carbon cycle. Low fCO_2 values along two transects indicated that much of the study area was a sink for atmospheric CO_2. The fCO_2 values were lowest near the Polar Front (PF) and the Subtropical Front (STF), concomitant with maxima of chlorophyll *a* and particulate and dissolved organic carbon. The largest biomass accumulations did not occur at fronts, which had high surface geostrophic velocities (20-51 cm s^{-1}), but in relatively low velocity regions near fronts or in an eddy. Thus vertical motion and horizontal advection associated with fronts may have replenished nutrients in surface waters but also dispersed phytoplankton. Although surface waters north of the PF have been characterized as a "high nutrient-low chlorophyll" region, low silicic acid (Si) concentrations (2-4 μM) may limit production of large diatoms and therefore the potential carbon flux. Low concentrations (4-10 μM Si) at depths of winter mixing constrain the level of Si replenishment to surface waters. It has been suggested that an increase in aeolian iron north of the PF may increase primary productivity and carbon export. Our results, however, indicate that while diatom growth and carbon export may be enhanced, the extent ultimately would be limited by the vertical supply of Si. South of the PF, the primary mechanism by which carbon is exported to deep water appears to be through diatom flux. We suggest that north of the PF, particulate and dissolved carbon may be exported primarily to intermediate depths through subduction and diapycnal mixing associated with Subantarctic Mode Water and Antarctic Intermediate Water formation. These physical-biological interactions and Si dynamics should be included in future biogeochemical models to provide a more accurate prediction of carbon flux.

1. Introduction

Recent models and observational studies suggest that the Southern Ocean is an important site for sequestering atmospheric carbon dioxide [*Sarmiento and LeQuéré,* 1996; *Takahashi et al.*, 1997]. This sequestration is a result of the interaction of physical and biological processes, such as intermediate and deepwater formation, deep convective mixing, subduction, and the solubility and biological carbon pumps [*Chen*, 1982; *Longhurst*, 1991; *Hoppema et al.*, 1995; *Sabine and Key*, 1998; *Sloyan and Rintoul*, 2001]. Air-sea CO_2 exchange is enhanced in the Southern Ocean because of relatively high wind speeds and a greater solubility of CO_2 at low seawater temperatures. The transfer of the relatively high concentrations of CO_2 in cold surface water to depth (i.e., the solubility pump) primarily is governed by physical processes, such as deep mixing and subduction of surface water to intermediate depths. Biota also influence the CO_2 flux through the uptake of inorganic carbon and the production of particulate and dissolved organic carbon and carbonate in the surface layer and the subsequent removal to deep water (i.e., the biological carbon pump). Particulate carbon is transferred from the surface layer through gravitational settling or by vertically migrating organisms, whereas dissolved organic carbon primarily is transported to depth by physical processes similar to that of dissolved inorganic carbon. The importance of the Southern Ocean as a net sink or source (e.g., upwelling at the Antarctic Divergence) for atmospheric CO_2 is uncertain because regional and seasonal changes in physical and biologi-

[1]Department of Ecology and Evolutionary Biology, University of Tennessee, Knoxville, Tennessee.
[2]Now at College of Marine Science, University of South Florida, Florida.
[3]Virginia Institute of Marine Science, College of William and Mary, Glouster Pt., Virginia.
[4]Pacific Marine Environmental Laboratory, Seattle, Washington.
[5]Grice Marine Lab, University of Charleston, Charleston, South Carolina.
[6]Now at Haskin Shellfish Research Laboratory, Port Norris, New Jersey.
[7]Joint Institute for the Study of Atmosphere and Ocean, University of Washington, Seattle, Washington.
[8]Bermuda Biological Station for Research, St. Georges, Bermuda.
[9]Now at Rosenstiel School of Marine and Atmospheric Science, University of Miami, Miami, Florida.
[10]Cooperative Institute for Marine and Atmospheric Studies, Rosenstiel School of Marine and Atmospheric Science, University of Miami, Miami, Florida.

Paper number 1999JC000090.
0148-0227/01/1999JC000090$09.00

cal processes controlling the air-sea exchange of CO_2 and carbon sequestration in the ocean are poorly known. The results presented here for the southwest Pacific Sector of the Antarctic Circumpolar Current (ACC) indicate that both physical and biological processes are important factors influencing carbon flux during summer.

The hydrography of the Pacific sector of the Southern Ocean is characterized by a series of meridional fronts; these fronts generally circle the Antarctic continent and define the ACC [*Orsi et al.,* 1995]. The ACC plays a very important role in global ocean circulation. It accounts for ~10% of the global ocean surface area, connects all major ocean basins, and is a major region for water mass formation and modification. From north to south the Subtropical Front (STF) is found within the Subtropical Convergence. All waters south of the STF are considered as part of the Southern Ocean. The eastward flowing ACC, driven by strong prevailing westerly winds, contains two major fronts: the Subantarctic Front (SAF) and the Polar Front (PF), which indicates the location of the Antarctic Convergence. The Subantarctic Zone lies between the STF and the SAF. The Polar Frontal Zone lies between the SAF and the PF. Between the PF and the continental water boundary is the Antarctic Zone, which contains the southern boundary (i.e., the Southern Front) of the ACC and the Antarctic Divergence. The band of westerly winds drives a northward Ekman flow, with surface divergence (hence upwelling) to the south of the wind stress maximum and surface convergence (hence downwelling) to the north. The positions of these fronts vary temporally and spatially, affected by such features as variable bathymetry and mesocale eddies [*Gille*, 1994; *Moore et al.,* 1999a]. Seasonal sea ice, which strongly influences much of the Antarctic Zone, seldom extends as far north as the Polar Front during winter [*Comiso et al.,* 1993].

The role of the solubility pump versus the biological pump in the Southern Ocean varies seasonally and by location. The solubility pump is governed by the air-sea flux of CO_2, which is a function of the difference in the fugacity of CO_2 (fCO_2) at the air-sea boundary and the gas transfer velocity [*Sabine and Key*, 1998]. In turn, gas solubility in the ocean depends largely on temperature and salinity [*Weiss*, 1974], and the transfer velocity depends on wind speed [*Sabine and Key*, 1998]. Thus regional and seasonal differences in CO_2 transfer to or from the ocean are influenced by upwelling, seasonal warming/cooling of surface waters, the timing and extent of sea ice, and weather. The biological pump (i.e., biological production and carbon export) is governed by seasonal changes in irradiance and ice cover, mixing processes and advection, macronutrient and micronutrient concentrations, and food web structure and dynamics [*Jacques*, 1989; *Nelson and Smith*, 1991; *de Baar et al.*, 1995]. The interplay of these two carbon pumps controls the regional and vertical partitioning of carbon pools.

Physical processes which effect CO_2 transfer from the surface layer to deeper water in the ACC include Subantarctic Mode Water (SAMW) and Antarctic Intermediate Water (AAIW) formation. SAMW forms during late winter convection, but this water sinks only to intermediate depths and north of the Subantarctic Front [*McCartney,* 1977, 1982]. *McCartney* [1977, 1982] argues that AAIW is an extreme variety of SAMW. AAIW, however, also may be ventilated by subduction throughout the year, primarily north of the Polar Front [*Molinelli*, 1981; *Piola and Georgi*, 1982], and therefore the biological pump may have an important influence on the carbon content of this water mass. A recent investigation of SAMW/AAIW cycling confirms that winter convection, subduction, and diapycnal mixing all play a role in the renewal and formation of these water masses [*Sloyan and Rintoul*, 2001]. Analyses of chlorofluorocarbon (CFC) data [*Fine*, 1993; *Wijffels et al.*, 1996] suggest that the SAMW and especially the AAIW may remain isolated from atmospheric exchange for at least decades before being upwelled as Upper Deep Water in the Antarctic. Hence these waters may play a significant role in the removal of anthropogenic atmospheric CO_2.

Despite the potential importance of this region to the global carbon cycle, few studies [e.g., *El-Sayed*, 1970; *Holm-Hansen et al.*, 1977; *Yamaguchi et al.,* 1985] have investigated the hydrography in relation to the distribution of nutrients and carbon pools in the Pacific sector of the ACC, and our knowledge about factors which control C cycling is very limited. The PF is known as one of the world's largest sites of accumulation of siliceous deposits, implying a relatively high production of diatoms [*Tréguer et al.,* 1997], yet evidence of high production in the ACC remains equivocal. *Banse* [1996] designated the Pacific Polar Frontal and Subantarctic Zones as high nutrient-low chlorophyll (HNLC) regions, and *Boyd et al.* [1999] extended this classification to a low-silicate regime as well. Low concentrations of bioavailable iron also may limit production [*Martin*, 1990; *de Baar et al.*, 1995; *Boyd et al.*, 2000]. Furthermore, sediment cores indicate that increases in aeolian iron dust during glacial periods increased carbon flux and presumably CO_2 drawdown in the ACC [*Kumar et al.,* 1995]. Despite the evidence of persistent low biomass in the modern ocean, *Murphy et al.* [1991] and *Sabine and Key* [1998] both observed CO_2 undersaturation in surface waters relative to that in the atmosphere in this region. They suggested that biological as well as physical processes significantly influence the CO_2 distribution in the southwest Pacific sector of the ACC.

As part of the World Ocean Circulation Experiment (WOCE) and the Joint Global Ocean Flux Study (JGOFS), a cruise was conducted in the Pacific sector of the Southern Ocean, in part to assess the region's role in the carbon cycle and to quantify the distributions of the various pools of carbon. This paper reports the distribution of hydrographic variables, nutrients, and dissolved and particulate carbon pools and describes the processes important to producing those distributions. Strong latitudinal gradients in the physical and chemical environment are a common feature in all sectors of the ACC [*Gordon and Mollinelli*, 1982], while dynamic mesoscale processes contribute to meridional variability [*Moore et al.*, 1999a]. The implications of the latitudinal gradients for carbon cycling and export are discussed.

2. Methods

WOCE hydrographic sections P14S (~172°E) and P15S (170°W) were sampled for a suite of physical, chemical, and biological measurements from the NOAA Ship *Discoverer* in the southwest Pacific Ocean between January 5 and February 4, 1996 (Figure 1). Hydrographic data were submitted to WOCE (http://diu.cms.udel.edu/woce), and all data were submitted to the Carbon Dioxide Information Analysis Center

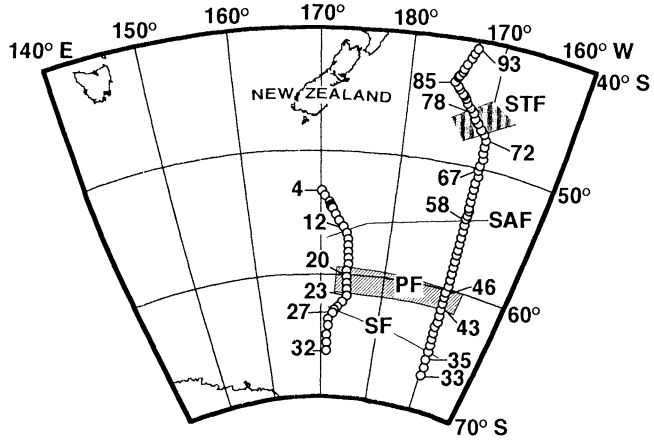

Figure 1. Map showing the location of stations (numbers) along World Ocean Circulation Experiment (WOCE) hydrographic sections P14S (170°- 174° E) and P15S (170° W) in the southwest Pacific sector of the Southern Ocean.
The Antarctic Circumpolar Current is located between the Subtropical Front and the Southern Front. The approximate locations of fronts are indicated (see text for criteria for selection of locations). STF, Subtropical Front; SAF, Subantarctic Front; PF, Polar Front; SF, Southern Front.

(CDIAC; http://cdiac.esd.ornl.gov). The hydrographic sections encompassed the Antarctic Zone (i.e., the Ross Sea Gyre), the Southern Front (SF), the PF, the SAF, and the STF. The identification and designation of physical features follows the methodology and terminology of *Orsi et al.* [1995]. Stations were occupied at a nominal spacing of 30 nautical miles (~55 km) from north to south on the first transect (P14S) and from south to north on the second transect (P15S).

At each station, continuous vertical profiles of temperature (± 0.002°C), salinity (± 0.002), and dissolved oxygen concentration (±1%) were obtained using Sea-Bird Electronics 911+ Conductivity-Temperature-Depth (CTD) sensors mounted on two different frames (a primary 36-position frame with 10-L bottles and a 24-position frame with 4-L bottles that was deployed only in heavy weather; [*McTaggart and Johnson,* 1997]). In situ oxygen samples were routinely collected during CTD/O_2 profiles and used for postmeasurement calibration of the O_2 sensor data following protocols described by *McTaggart and Johnson* [1997]. Geostrophic velocities were calculated assuming zero velocity at the deepest common level of each station pair (4000 dbar). One exception was stations 25-26, where velocities were referenced to zero velocity at 2650 dbar since the lateral density gradient below this level is supported by a topographic feature unresolved by the station spacing. The Niskin bottles were closed at selected pressures during the CTD upcast. Among a number of different measurements, water samples from these bottles were analyzed for salinity, dissolved inorganic nutrient concentrations (nitrate, phosphate, and silicic acid), total dissolved inorganic carbon (TCO_2), and total organic carbon (TOC).

Owing to time constraints, only one cast per day was made for biological measurements, resulting in station spacing of 90 to 120 nm (165-220 km). Just before dawn, water was sampled from either 10-L Niskin or 30-L Go-Flo bottles (both fitted with Teflon-coated, stainless steel springs) hung on a Kevlar line. Subsamples were collected for phytoplankton pigments, nutrients (including ammonium and urea), particulate organic matter, and primary productivity. Irradiance attenuation (i.e., light levels experienced by phytoplankton) was calculated from spectroradiometer (MER 500; BioSpherical Instruments) profiles conducted each day at local noon. Sampling depths within the euphotic zone (100, 50, 30, 15, 5, 1.0, and 0.1% of surface irradiance; between 75 and 150 m) were estimated from the water column attenuation determinations made on the previous day. One additional depth below the euphotic zone between 100 and 200 m also was sampled.

Dissolved phosphate, silicic acid, and nitrate were analyzed using protocols of *Gordon et al.* [1993]. All vials and caps were rinsed with 10% HCl prior to each station and rinsed at least three times with sample water before filling. Samples usually were analyzed immediately but were occasionally stored for up to 12 hours at 4°-6°C. Samples were analyzed using an Alpkem RFA 300 modified with a Spectro-100 UV/VIS detectors (Thermo Separation Products); all analyses were within the linear range of the instrument. Concentrations were converted to μmol kg^{-1} by calculating sample densities using IPTS-68 laboratory temperatures and PSS-78 bottle salinities [*UNESCO,* 1981]. Analytical precision was determined from replicate analyses (two to seven measurements) on one or more samples for almost every station. Average standard deviations (μmol kg^{-1}) were 0.008 for phosphate (n = 205), 0.08 for silicic acid (n = 407), 0.05 for nitrate (n = 378), and 0.003 for nitrite (n = 15 for samples > 0.05 μmol kg^{-1}).

Samples for urea and ammonium were collected into clean sample bottles and refrigerated until analysis (usually within 2-4 hours). Urea measurements were made using an adaptation of the colorometric method described by *Mulvenna and Savidge* [1992] based on the reaction of urea with diacetylmonoxime. Ammonium measurements were made following the colorometric method described by *Parsons et al.* [1984]. Both analyses were performed on triplicate 25-mL aliquots, with the reaction carried out in acid-cleaned screw-capped glass culture tubes. Absorbances were measured in 5-cm quartz cells using a Shimadzu Model 1601 spectrophotometer. Limits of detection were 0.1-0.2 μM for both urea-nitrogen and ammonium.

TCO_2 was analyzed by coulometric titration with a SOMMA system following the method outlined by *Lamb et al.* [1997]. The fCO_2 was measured by equilibrating the seawater samples at 20°C with a headspace, followed by measuring the fCO_2 in the headspace with a LI-COR nondispersive infrared analyzer [*Wanninkhof and Thoning*, 1993]. Surface sample values of fCO_2 were corrected to in situ temperatures to determine the direction of air-sea exchange. TOC, which includes both suspended and dissolved organic carbon, was analyzed by the high-temperature combustion method as described by *Doval and Hansell* [2000]. All TOC concentrations were referenced to Sargasso Sea water collected at 2600 m and corrected for a system blank provided by J. Sharp (University of Delaware) as well as an instrument blank. Standard deviations of replicate TOC measurements were ± 2%.

Chlorophyll *a* was quantified by high performance liquid chromatography (HPLC). Approximately 1-4 L of seawater was filtered through Whatman GF/F filters at a vacuum pressure of < 125 mm Hg. Filters were stored in liquid nitrogen

until processing on shore. In the laboratory, filters were ground and extracted in 90% cold acetone. Pigment concentrations were measured on a Hewlet-Packard 1050 Series HPLC with a Phenomonex Sphericlone ODS(2) reverse-phase column using a quaternary gradient to separate and identify the pigments. The gradient elution program was modified from *Wright et al.* [1991]. The HPLC system was calibrated using known concentrations of pigments extracted from unialgal cultures. The coefficient of variation for replicate standards was < 3%.

Particulate organic carbon (POC) and nitrogen (PON) samples (0.5-1 L) were filtered through a combusted (450°C for 2 hours) GF/F filter under low vacuum, then rinsed with a small amount (~0.1 mL) of 1.0 *N* HCl in filtered seawater to remove inorganic carbonates. The filters were dried at 60°C and analyzed for carbon and nitrogen content with a Carlo-Erba Model EA1108 elemental analyzer after high-temperature pyrolysis using acetanilide as a standard. An average blank (refiltered filtrate) value, determined from both surface and bottom depth samples, was subtracted from all measured values for each cast.

3. Results

The latitudinal hydrographic fronts and associated physical processes in the ACC are important in governing gradients of nutrients and biology. First, we describe the location of the fronts and then the zonal and meridional variability in environmental conditions and patterns of nutrient and carbon pool distributions.

3.1. Location of Fronts

The hydrographic fronts are persistent features in all sectors of the ACC; their zonal location may vary depending on regional bathymetry and circulation. The locations of fronts was determined using a number of hydrographic properties (Table 1) [*Orsi et al.,* 1995]. While the emphasis here is on the near-surface layer, water mass indicators of fronts occur over a range of depths (from near surface to as deep as 800 m). Surface geostrophic velocity also may be used as a frontal position indicator. In the Southern Ocean this quantity is traditionally the result of vertical integration of density over much, if not all, of the water column. Here we identify the front locations from south to north in both P14S and P15S.

The SF can be discerned by three water properties (Table 1) and geostrophic velocity. Abrupt transitions in potential temperature (θ, Figures 2a and 2b), salinity (Figures 2c and 2d), oxygen (Figures 3a and 3b), and density (Figures 3c and 3d) were observed between stations 26 and 27 (~63°S) on P14S; surface geostrophic velocity also exceeded 23 cm s^{-1}, another indicator that the SF was at that site (Figure 4a). Along P15S, geostrophic velocities reached 10 cm s^{-1} between stations 35 and 36 (~66°S) and 16 cm s^{-1} between stations 43 and 44 (~61°S; Figure 4b), and θ indicators suggested that the SF was split between a southern and northern branch at these station pairs. The northern branch may have been combined with a southern branch of the Polar Front as argued below.

The PF can be demarcated using θ (Table 1) and geostrophic velocities, both of which suggested bifurcation. However, fine structure in the θ profiles made the use of the depth of θ_{min} criteria problematic, presumably because of interleaving around the front. On P14S the PF appeared to have a southern branch between stations 23 and 24 (~61.5°S) and a northern branch between stations 19 and 20 (~59.5°S). On P15S a southern branch, perhaps combined with a northern branch of the SF, may have existed between stations 43 and 44, but the most likely location for the PF was between stations 46 and 47 (~59.5°S). On P14S, geostrophic velocity exceeded 25 cm s^{-1} between stations 23 and 24 and 27 cm s^{-1} between stations 19 and 20, and on P15S it reached 16 cm s^{-1} between stations 43 and 44 and 18 cm s^{-1} between stations 46 and 47 (Figure 4).

The SAF can be identified by three water properties (Table 1) and geostrophic velocity, but eddies or meanders made SAF locations ambiguous. Salinities > 34.2 above 300 m were observed between stations 13 and 14 on P14S and stations 58 and 59 on P15S (Figures 2c and 2d), and θ > 5°C at 400 m was found between stations 13 and 12 in P14S and stations 58 and 59 on P15S (Figures 2a and 2b). Oxygen concentrations (Figures 3a and 3b) decreased below 305 μmol kg^{-1} above 200 m between stations 14 and 15 on P14S and between stations 55 and 56 on P15S, although such low levels did not persist until between stations 52 and 53. On P14S, station 9 also met the *S* and θ indicators for delineation of the SAF. Finally, geostrophic velocity exceeded 49 cm s^{-1} be-

Table 1. Summary of Hydrographic Properties Used to Define the Various Fronts in the Southern Ocean[a]

Front	Potential Temperature, θ°C	Salinity	Oxygen, μmol kg^{-1}
Southern Front	> 1.8 at z > 500 m	34.73 at z > 800 m	< 185 at z > 500 m
Southern Front	< 0.0 at z < 150 m		
Polar Front	< 2.0 at z < 200 m		
Polar Front	θ_{min} at z > 200 m		
Polar Front	> 2.2 at z > 800 m		
Subantarctic Front	> 4-5 at z = 400 m	< 34.2 at z < 300 m	> 305 at z < 200 m
Subtropical Front	> 12.0 at z = 100 m	> 35 at z = 100 m	

[a]After Orsi et al. [1995].

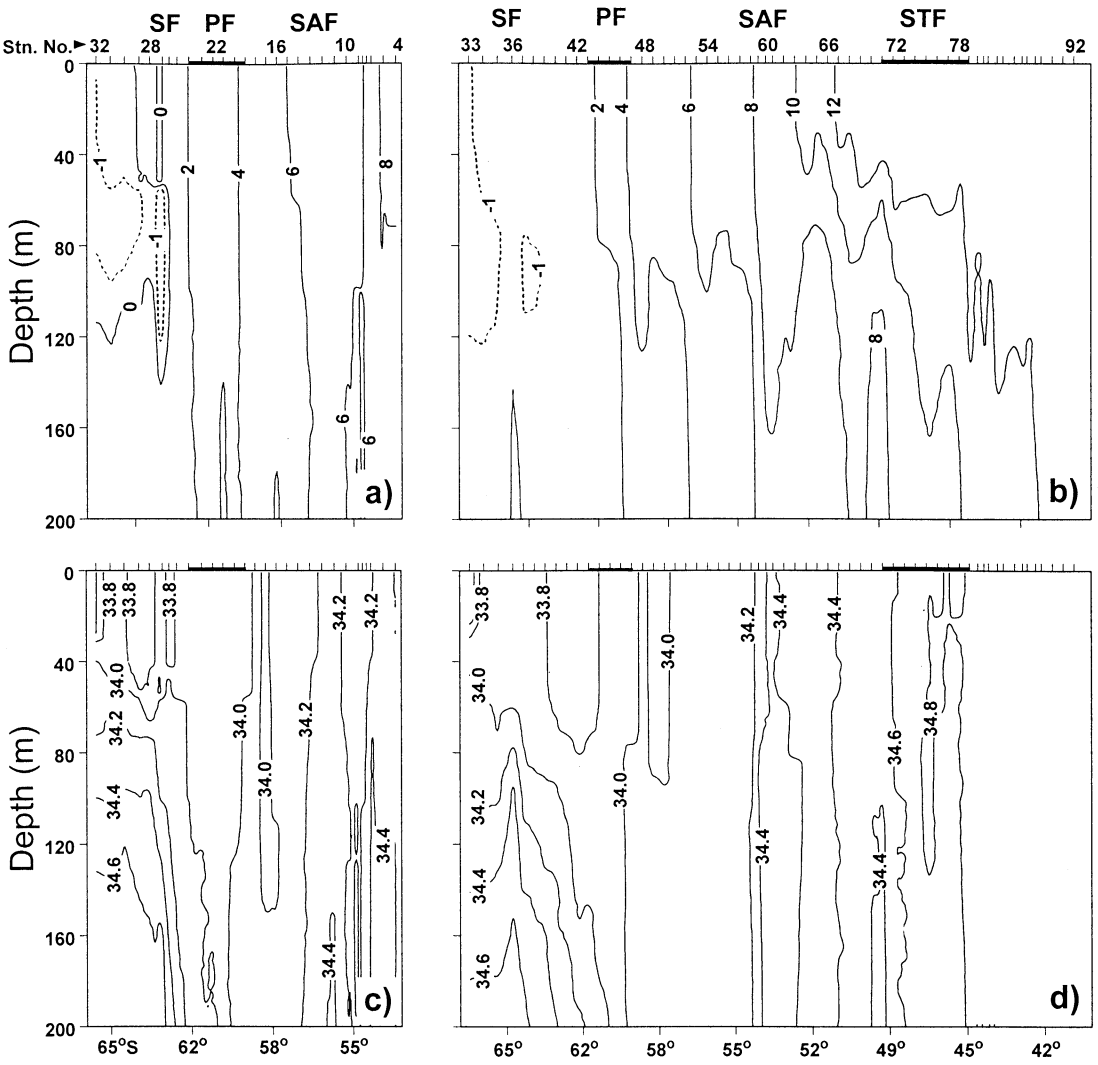

Figure 2. The distribution of (a and b) potential temperature (°C) and (c and d) salinity. Data are continuous measurements from conductivity-temperature-depth (CTD) profiles. Here and in Figures 3-9 the locations of the Southern Front (SF), the Polar Front (PF), the Subantarctic Front (SAF), and the Subtropical Front (STF) and station numbers are indicated above the top panels; the dark bar under PF and STF indicates the northern and southern branches of these fronts; latitude (°S) is shown below the bottom panels. Left and right panels are hydrographic sections P14S and P15S, respectively.

tween stations 8 and 9, -25 cm s^{-1} between station 10 and 11, and 27 cm s^{-1} between stations 13 and 12 for P14S (Figure 4a). On P15S, velocities exceeded 51 cm s^{-1} between stations 58 and 59, -18 cm s^{-1} between stations 62 and 63, and 29 cm s^{-1} between stations 66 and 67 (Figure 4b). These combined results suggests that the SAF probably was located between stations 12 and 13 (~56°S) on P14S, south of a cold-core eddy centered around station 9. For P15S the water properties placed the SAF between stations 58 and 59 (~54°S), at the strongest geostrophic velocity. The feature to the north was probably a cold-core eddy centered about station 65.

Finally, STF can be located using θ and *S* (Table 1) with geostrophic velocity. The STF occurred north of P14S (near-surface temperatures never exceed 10 °C; Figure 2a), whereas on P15S STF, indicators were spread over a wide band between stations 72 and 81 (47.5°-44°S). Geostrophic velocities (Figure 4) were high between stations 71 and 72 (24 cm s^{-1}), and between stations 78 and 79 (22 cm s^{-1}), either or both of which could be associated with the broad convergence zone.

The vertical stratification, expressed as Brunt-Väisälä frequency, showed marked variations on P14S and P15S (Figure 5). The upper water column was relatively stable in near-surface waters (20-40 m) at the southernmost stations in the Antarctic Zone on both transects. Low-density meltwater from winter sea ice contributed to this stability. On P14S the greatest stratification was associated with the lowest mean geostrophic velocities south of the SF. Near the PF the upper 40 m were well mixed with increasing stability between 40 and 60 m depth, although P15S stations were less stable than P14S stations at these depths. Both transects were weakly stratified in the Polar Frontal Zone (56°-61.5°S; 54°-61.5°S), a transition region where subduction occurs. P15S stations showed increasing stratification in the upper 80 m near the STF owing to seasonal warming of surface water.

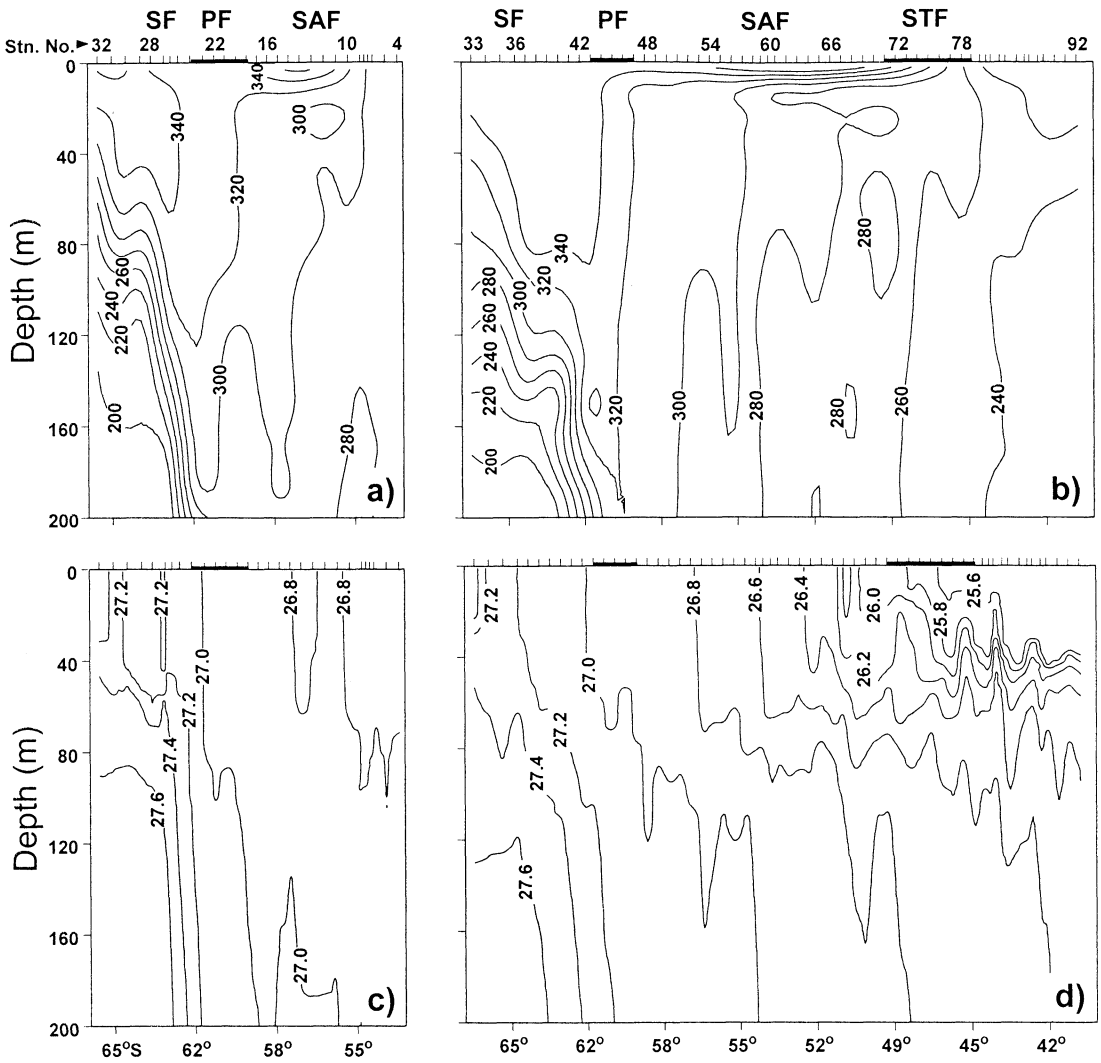

Figure 3. The distribution of (a and b) oxygen (μmol kg^{-1}) and (c and d) density (expressed as σ_T). Left and right panels are hydrographic sections P14S and P15S, respectively.

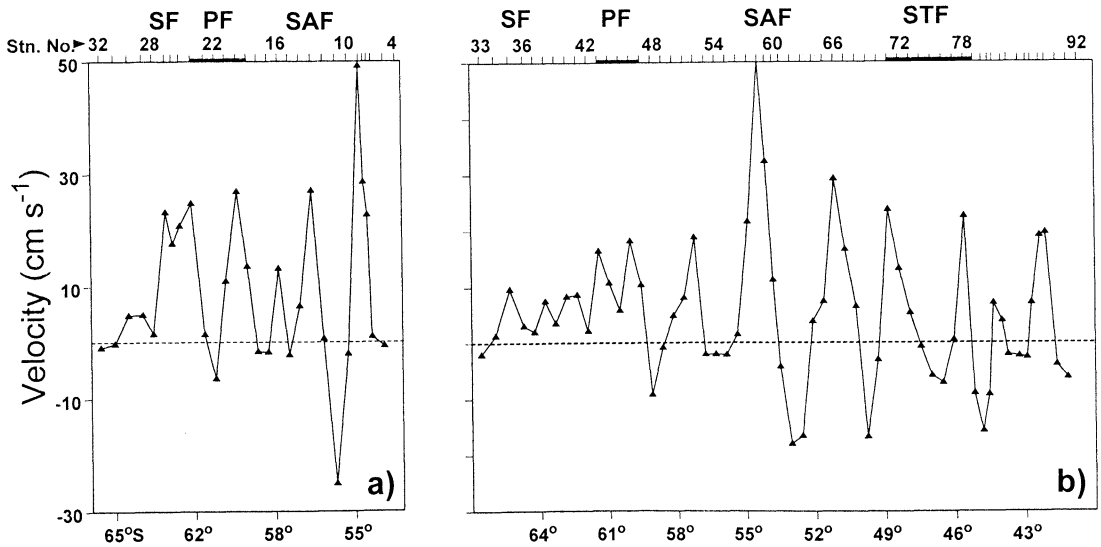

Figure 4. Calculated surface geostrophic velocities along (a) P14S and (b) P15S. All velocities were calculated relative to 4000 dbar, except for stations 25-26, which were referenced to 2650 dbar. Velocities were assumed to be zero at the deepest common level of each station pair.

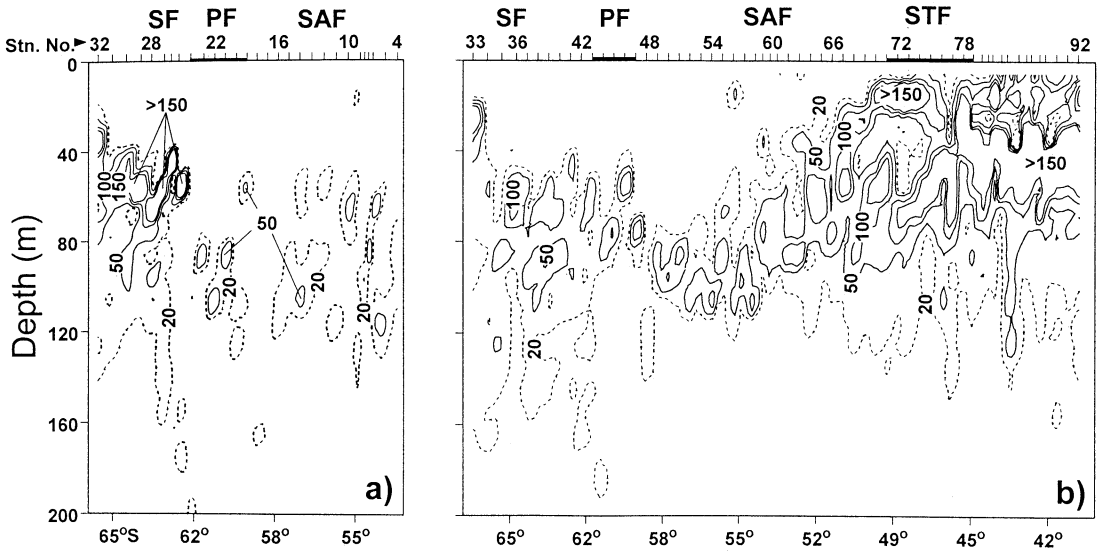

Figure 5. Calculated Brunt-Väisälä or buoyancy frequency N^2 along (a) P14S and (b) P15S. The buoyancy frequency was filtered with a 21 dbar (8 dbar half width) Blackman filter.

3.2. Nutrient and Particulate and Dissolved Carbon Distributions

Weather conditions (e.g., wind speed and sea state) influence air-sea CO_2 exchange. These factors, along with cloudiness and day length, also influence the daily integrated irradiance experienced by phytoplankton in the surface mixed layer. Although photoperiods were 24 hours at the southernmost stations, weather conditions were poor, consisting of overcast skies and relatively high sustained winds and sea state (Table 2). Photoperiods decreased to 20 hours at the PF with similar weather conditions. Photoperiods were 15 hours at the northern stations in the subtropical gyre, but weather conditions were more favorable, with partly cloudy skies, lower wind speed, and calmer seas. The depth of the euphotic zone, defined as the depth to which 0.1% of surface irradiance penetrated, was shallowest in the PF (~50 m) and deepest in the Subantarctic Frontal Zone (125 m). Photosynthetically active radiation (PAR) ranged from 180 to 1410 μmol photon m^{-2} s^{-1} over the study area (Table 2).

Nitrate concentrations were relatively high (30 μ*M*) throughout the upper 200 m of the water column in Antarctic waters and gradually decreased to the north across the ACC to relatively low concentrations (< 5 μ*M*) in the upper 60 m near the STF (Figure 6b). Relatively low concentrations of both ammonium (mean 0.26 ± 0.27 μ*M*; n = 137; range 0-1.56) and urea (mean 0.23 ± 0.21 μ*M*; n = 123; range 0-0.88) also were present at all stations (Figures 6c-6f, respectively). Ammonium maxima tended to occur between 50 and 140 m near frontal features. Distributions of urea were different from those of ammonium. The highest urea concentrations occurred in the upper 20 m in the vicinity of and south of the PF as well as in deeper waters (> 140 m) at the PF. Both ammonium and urea concentrations were low (~0.2 μ*M*) in the upper 50 m from the Polar Frontal Zone north to the subtropical gyre.

Phosphate concentrations ranged from 0.06 to 2.12 μ*M*, with the highest concentrations being observed in Antarctic waters (Figures 7a and 7b). Although concentrations remained relatively high between the PF and the SAF (> 1.4 μ*M*), they decreased northward to < 1.0 μ*M*. The lowest concentrations (< 0.1 μ*M*) occurred in surface waters (0-15 m) north of the SAF. Relatively high silicic acid concentrations (20-80 μ*M*) only occurred south of the PF (Figures 7c and 7d). There was a sharp gradient at the PF, and all stations north of the PF had low silicic acid concentrations (< 4 μ*M*) in the upper 80 m of the water column.

TCO_2 inventories ranged from 2255 μmol kg^{-1} in colder southern waters to 2024 μmol kg^{-1} in warmer waters to the north (Figures 8a and 8b). The lowest concentrations were in the relatively warm surface waters north of the STF, following solubility constraints. Total (dissolved plus particulate) organic carbon concentrations ranged from < 42 μmol kg^{-1} in deep waters (> 200 m) to > 80 μmol kg^{-1} in the surface layer of subtropical waters (Figures 8c and 8d). The mean surface (< 50 m) TOC concentration in P14S was 53.2 μmol kg^{-1}, whereas in P15S it was 61.8 μmol kg^{-1}. No strong spatial trends in TOC concentrations were observed. On P14S, increased concentrations occurred near the surface south of the SF and in the vicinity of the eddy at station 9. On P15S, values were elevated in the SF and increased between the SAF and the STF. Because deepwater dissolved organic carbon concentrations in this region are ~42 μmol kg^{-1} (Figures 8c and 8d) [see also *Hansell and Carlson*, 1998], the surface increase in TOC represents a sizable pool of organic matter. We have no information on the turnover of this pool or the winter concentrations in this region; therefore estimates of net production cannot be made conclusively.

CO_2 fugacity (fCO_2) in surface waters did not show the same latitudinal trend across the ACC (Figures 9a and 9b) as that of TCO_2 (Figures 8a and 8b). Most of the region was characterized by fCO_2 values below atmospheric values (~350 μatm). The lowest values were observed on the P14S transect near the SF and the PF and on the P15S transect south of the PF and in the STF. The highest fCO_2 values (higher than atmospheric values) were observed near the SAF on both transects and in the vicinity of the SF on P15S. The lowest fCO_2 values occurred in the same areas as chlorophyll *a* (Figures 9c and 9d) and POC (Figures 9e and 9f) maxima.

Table 2. Weather Condition, Sea State, Euphotic Zone Depth, and Irradiance Along P15S

Station Number	Weather	Wind Speed, m s^{-1}	Wave Height, m	Euphotic Zone, m	PAR_{1200},[a] μmol m^{-2} s^{-1}
33	snow flurries	8.31	0.9 - 1.5	75	280
37	snow	15.6	3.1 - 3.7	75	280
41	fog, rain	10.4	1.2 - 1.8	50	970
44	rain	15.6 - 20.8	2.4 - 3.1	50	410
47	overcast	13.0 - 15.6	2.4 - 3.1	70	475
50	overcast	6.23	1.2 - 1.8	85	475
54	overcast	8.31	0.9 - 1.8	100	200
58	overcast	9.34	0.9 - 1.2	125	670
60	overcast	11.9	0.9 - 1.2	125	365
62	overcast	13.5	0.9 - 1.2	125	365
65	overcast	11.9	1.5 - 2.1	125	580
69	overcast	6.75	0.9 - 1.5	100	1390
72	fog	5.19	0.9 - 1.2	90	1410
76	fog	ND[b]	ND[b]	75	400
80	partly cloudy	8.31	0.6 - 0.9	100	730
86	partly cloudy	2.60	0.3 - 0.6	100	680
92	partly cloudy	6.75	0.6 - 0.9	105	205

[a]Photosynthetically active radiation (PAR) levels at the sea surface; data from F. Chavez (unpublished data, 1996).

[b]ND is no data.

Surface chlorophyll concentrations (100% I_o) averaged 0.25 and 0.43 μg L^{-1} on P14S and P15S, respectively (ranges 0.07-0.64 and 0.11-1.18 μg L^{-1}). On P14S the greatest phytoplankton biomass was observed between the north and south current cores of the PF (Figure 9c); a second maximum occurred below 100 m in an eddy at station 9. On P15S the greatest chlorophyll concentrations were found ~280 km south of the PF (Figure 9d). POC concentrations were highest in the upper 80 m of the water column, with maximum concentrations on each transect 14.1 μmol L^{-1} (station 12, 70 m) and 31.6 μmol L^{-1} (station 41, surface), respectively. The maximum POC concentration on P14S (Figure 9e) occurred on the northern side of the SAF in a region of low geostrophic velocity (Figure 4a). POC levels south of the SAF were relatively low, although there was a slight increase in POC concentration (> 10 μmol L^{-1}) at the PF coincident with the chlorophyll maximum. Along P15S a distinct maximum was observed ~280 km south of the PF (Figure 9f), which also correlated with the observed pigment maximum. POC contributed an average of 12.0 and 13.7% of the total organic carbon found in P14S and P15S, respectively.

4. Discussion

The role of the Southern Ocean in modulating atmospheric CO_2 is uncertain. Our present knowledge about factors which influence the solubility and biological C pumps limits our ability to predict how ocean circulation, mixing, and the composition and production of marine organisms will respond to climate forcing. In the following discussion, we compare our results on the direction of air-sea exchange of CO_2, as inferred from values of fCO_2, with those of previous studies and then examine the interplay of physical processes and nutrients which may have influenced the biological and solubility pumps in the export of carbon from the surface layer.

4.1. ACC as a Sink for Atmospheric CO_2

The pattern of dissolved inorganic carbon concentrations was influenced by both solubility and biological processes in our study area. In polar waters, TCO_2 concentrations were ~2150 μmol kg^{-1} near surface (temperatures < 0°C) and increased to ~2,255 μmol kg^{-1} below 200 m depth (Figures 8c and 8d). In subtropical waters, TCO_2 concentrations de-

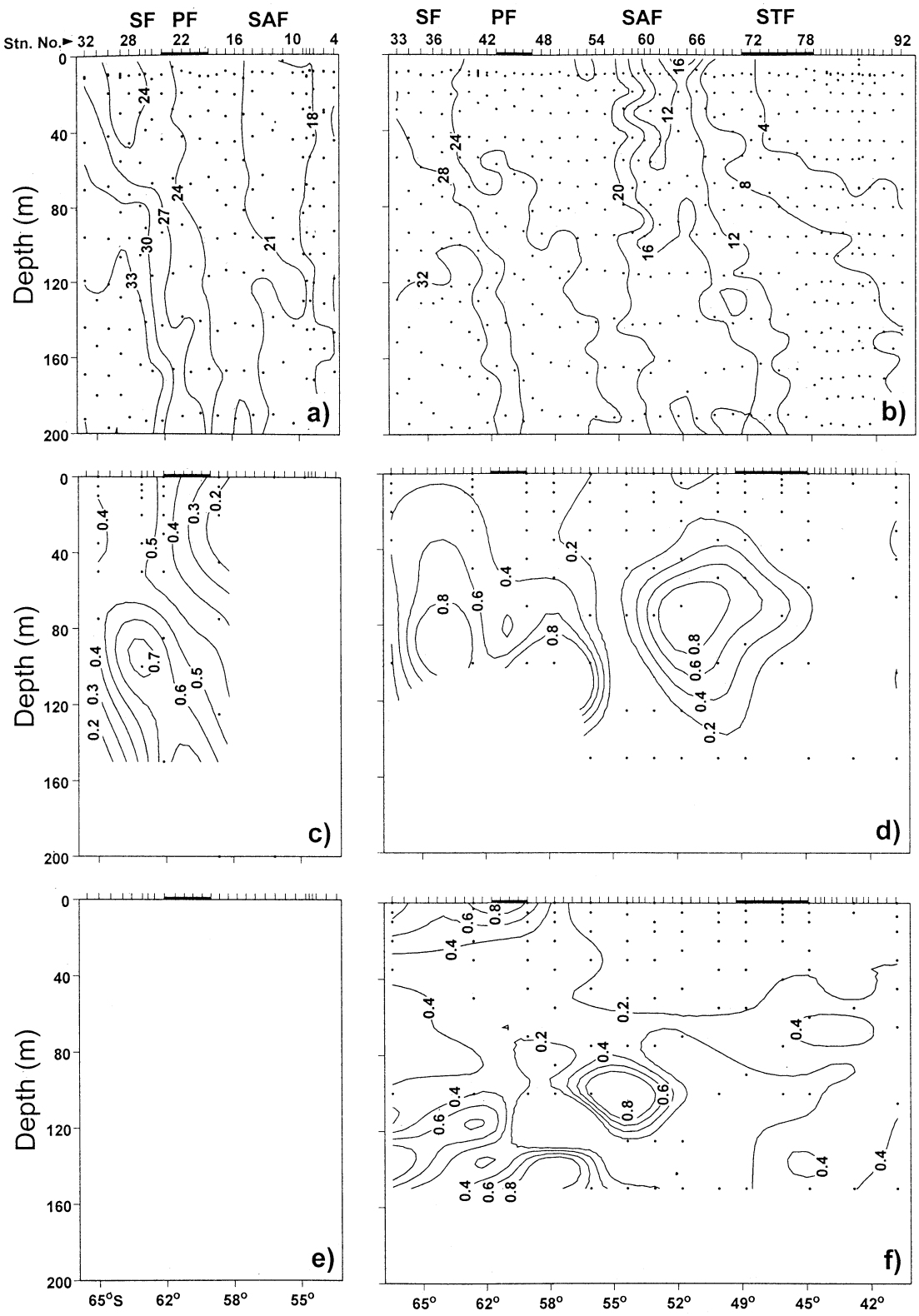

Figure 6. The distribution of (a and b) nitrate, and (c and d) ammonia, (e) no data, and (f) urea. Units are μmol kg^{-1}. Dots indicate depth of discrete measurements. Left and right panels are hydrographic sections P14S and P15S, respectively.

creased to < 2050 μmol kg^{-1} near surface (temperatures of 12°C). This decreasing trend is consistent with the temperature dependence of the solubility of dissolved CO_2 in seawater. Relatively low fCO_2 values concomitant with phytoplankton biomass maxima, however, indicate that biological processes were important as well (Figure 9).

The lowest fCO_2 values occurred at both the PF and the STF, suggesting that these sites were a net sink of atmos-

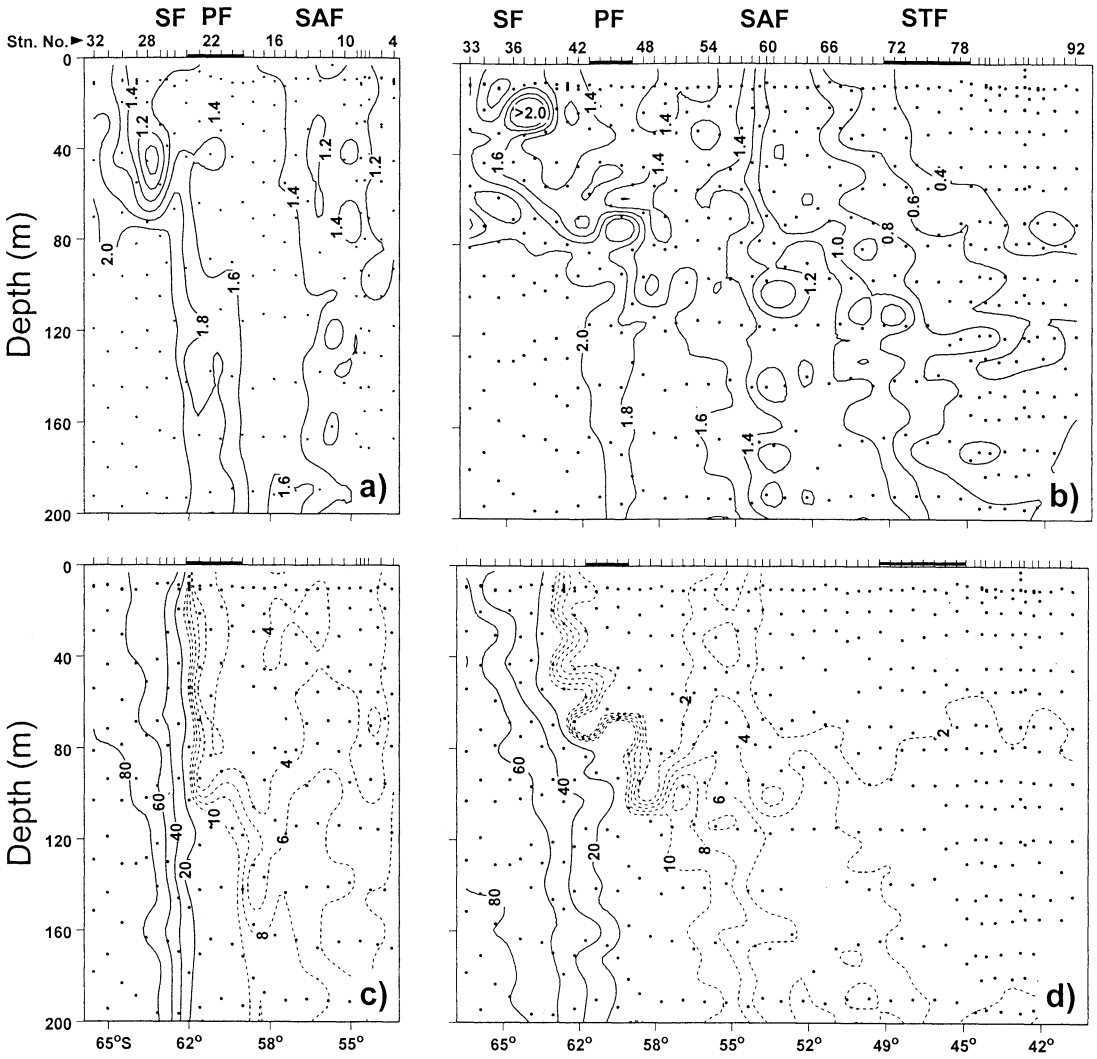

Figure 7. The distribution of (a and b) phosphate (μmol kg^{-1}) and (c and d) silicic acid (μmol kg^{-1}). Dots indicate depth of discrete measurements. Dotted contour indicates change in contour interval. Left and right panels are hydrographic sections P14S and P15S, respectively.

pheric CO_2. The highest concentrations of chlorophyll *a* and POC also occurred at these locations. In addition, the highest rates of surface (100% I_o) primary productivity on section P15S were observed at 62.5° and 64.5°S near the PF (0.163-0.167 μmol C L^{-1} h^{-1}) and at 46° and 49°S near the STF (0.094–0.115 μmol C L^{-1} h^{-1}) (K. Daly and W. Smith, unpublished data, 1996). Thus biological removal of CO_2 likely exceeded the flux owing to gas exchange or vertical and horizontal mixing. Relatively high fCO_2 values (~360 μatm) near the SAF suggest that this region may have been a net summertime source of CO_2, possibly resulting from seasonal warming of cold surface water advected northward in the Ekman layer. The spatial variability of net sources and sinks is illustrated by the low fCO_2 values observed near the SF on P14S, whereas relatively high values were observed on P15S, possibly due to upwelling at the southern boundary of the ACC.

The importance of the Southern Ocean as a sink for atmospheric CO_2 is uncertain owing to the limited number and variability of field observations. Recent studies, however, suggest that the STF and PF often are sinks for carbon during summer, even though these frontal regions are spatially and temporally variable. For example, *Sabine and Key* [1998] observed a CO_2 sink over a large section of the ACC in the eastern Pacific sector during summer, except for a small net source near the PF. In contrast to our findings, their largest sinks were near the SAF and south of the PF. *Murphy et al.* [1991] also observed undersaturation in surface waters with respect to the atmosphere between 50° and 60°S in the western Pacific sector of the ACC during autumn. *Metzl et al.* [1991] reported that the western section of the Indian Ocean sector of the ACC was a net source during summer, while the eastern section was a net sink. The largest sink was at the STF, with a smaller sink near the PF. *Clementson et al.* [1998] also observed undersaturation in surface waters between 40° and 51°S, which includes the STF, south of Australia during summer. *Bakker et al.* [1997] reported a sink at the PF in the Atlantic sector during spring. However, they estimated their study site was only a minor sink overall since other areas acted as a source because of seasonal warming ef-

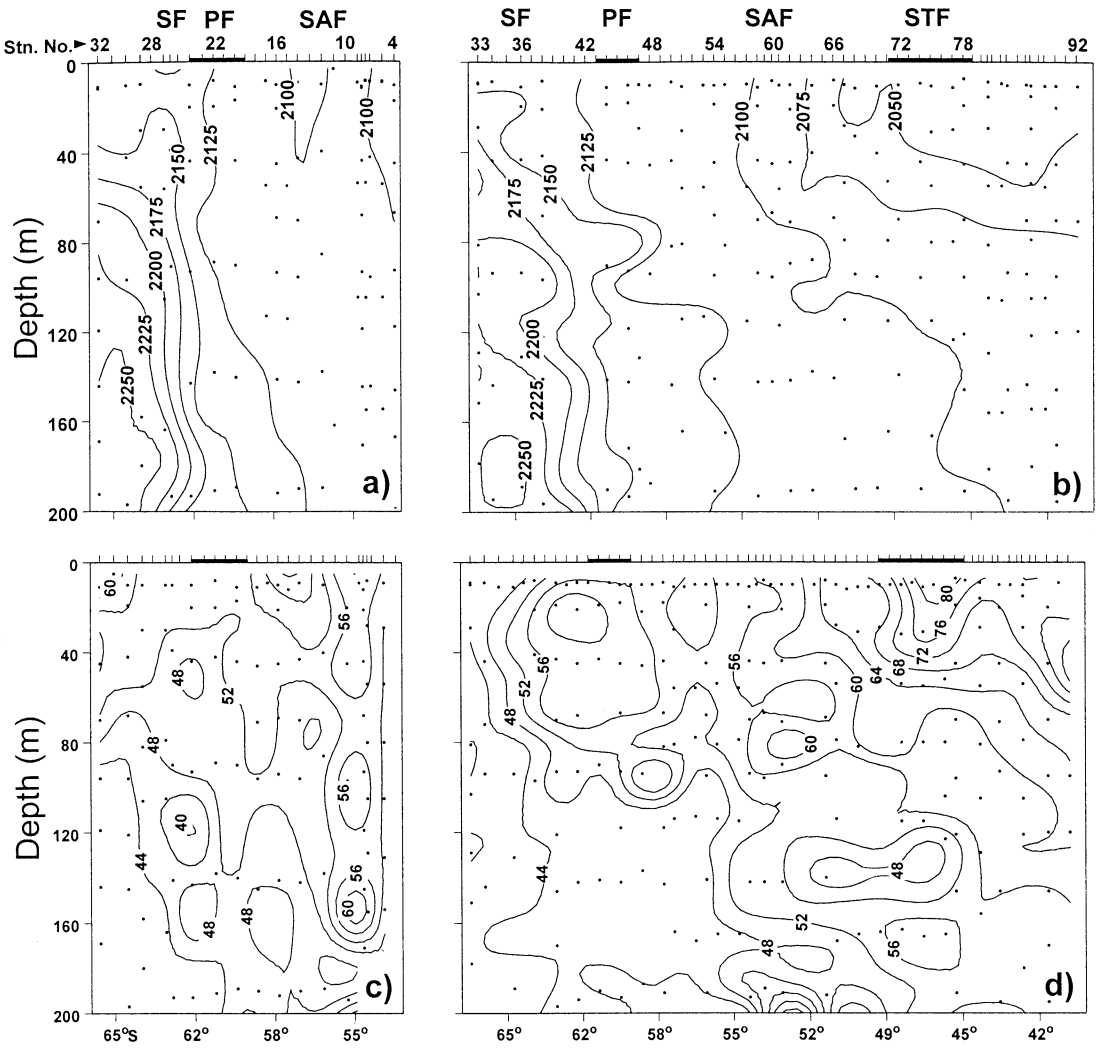

Figure 8. The distribution of (a and b) dissolved inorganic carbon (μmol kg^{-1}) and (c and d) total organic carbon (μmol kg^{-1}). Dots indicate depth of discrete measurements. Left and right panels are hydrographic sections P14S and P15S, respectively.

fects of surface water. In contrast to these studies, *Robertson and Watson* [1995] found that CO_2 was generally undersaturated in surface waters between early and late summer over a large area encompassing the southeast Pacific ACC, the Bellingshausen Sea, the eastern Atlantic, and Indian Ocean sectors. The only areas that acted as a CO_2 source to the atmosphere were near the SAF and the PF south of Africa. Although most of these studies suggested that biological activity influenced the CO_2 drawdown, the role of the biological pump remains poorly known.

4.2. Phytoplankton Biomass Distributions

High phytoplankton biomass detected by shipboard sampling or satellite ocean color sensors is often used to indicate high productivity. Low biomass, however, does not necessarily infer low productivity. Phytoplankton blooms are ephemeral features that require sufficient irradiance and nutrients to sustain growth and, in order for biomass to accumulate, growth rates must exceed losses due to advection, sinking, and grazing. The ACC between the STF and the PF has been characterized as a HNLC region [*Minas and Minas*, 1992; *Banse*, 1996]. Chlorophyll *a* concentrations (0.07–1.18 μg L^{-1}) observed during our study are typical of those reported previously for the Pacific sector [e.g., *El-Sayed*, 1970; *Holm-Hansen et al.*, 1977; *Banse*, 1996; *Boyd et al.*, 1999] as well as other sectors of the ACC [e.g., *Fukuchi*, 1980; *Yamaguchi et al.*, 1985; *Comiso et al.*, 1993].

Although low chlorophyll biomass is common, satellite data, which provide greater spatial and temporal resolution than ship-based studies, also indicate that transient blooms predictably occur in our study area. The maximum surface chlorophyll (chl) concentration detected by satellites near the PF during austral summer is ~3 μg L^{-1} [*Moore et al.*, 1999b], whereas elevated pigments rarely were detected in the Subantarctic Zone [*Banse and English*, 1997]. Substantial blooms (up to 8 μg chl L^{-1}) at the PF also have been reported from other regions [e.g., *Whitehouse et al.*, 1996; *Smetacek et al.*, 1997].

Past studies did not determine which factors governed algal growth or biomass in the Pacific PF region. In the Subantarctic Zone (between the SAF and the STF), *Boyd et al.* [1999] found that irradiance and Fe and Si limitation controlled algal

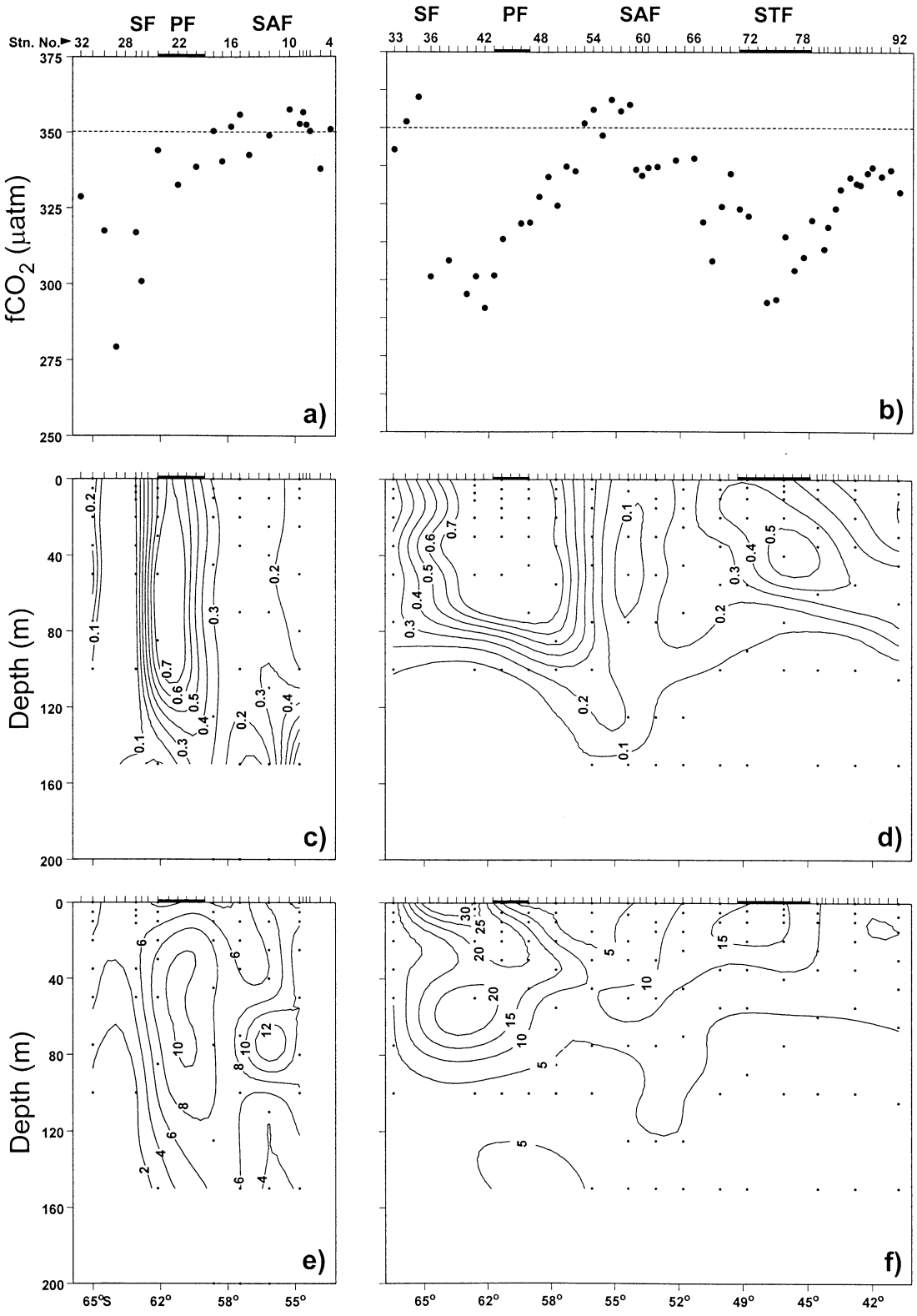

Figure 9. Distribution of (a and b) CO_2 fugacity (fCO_2, µatm) in surface waters and the distribution of (c and d) chlorophyll *a* (ug L^{-1}) and (e and f) particulate organic carbon (µmol L^{-1}) with depth. In Figures 9a and 9b, dotted line denotes the atmospheric value of fCO_2 for comparison. In panels 9c-9f, dots indicate the depth of discrete measurements. Left and right panels are hydrographic sections P14S and P15S, respectively.

growth, while *Banse* [1996] suggested that grazing maintained seasonal phytoplankton biomass at relatively low levels. *Bradford-Grieve et al.* [1999], however, reported that C:chl ratios are elevated in this region in spring, and therefore the apparent low biomass based on chlorophyll concentrations or satellite observations conceals an increase in carbon biomass not controlled by grazing.

4.3. Factors Controlling Phytoplankton Production and Biomass

The ACC is known to be a region with extensive spatial and temporal variability induced by meandering, eddies, and other mesoscale features [*Gordon and Molinelli,* 1982; *Nowlin and Klinck,* 1986; *Morrow et al.*, 1992; *Moore et al.,* 1999a, 1999b]. In the southwest Pacific sector, seasonal variations in the location of the PF are small [*Moore et al.,* 1999a], with the mean flow in this region being bathymetrically steered by the Pacific-Antarctic Ridge [*Orsi et al.,* 1995]. In locations where bottom topography constrains the flow, such as in the southwest Pacific, surface velocities intensify, and baroclinic instabilities lead to increased eddy activity.

Although there are few field studies of the SAF in the southwest Pacific (reviewed by *Banse and English* [1997]); Geosat altimeter data indicate that meridional meanders and eddy activity are common in both the PF and the SAF over 17-day intervals [*Gille and Kelly*, 1996]. Maps of root-mean-square sea surface height variability from TOPEX/Poseidon satellite altimeter data also suggest that eddies are a common feature in this region [*Wunsch and Stammer*, 1995]. Cold-core eddies have been reported in the Subantarctic Zone south of New Zealand [*Piola and Georgi*, 1982], consistent with our findings, as well as below Australia [*Rintoul et al.*, 1997] and in the Indian Ocean sector [*Reed and Pollard*, 1993]. The flow of the STF in the southwest Pacific is influenced by the bathymetry of the Campbell Plateau and the Chatham Rise to the east of New Zealand [*Garner*, 1959; *Heath*, 1985]. The STF in this region also appears to be an area of high eddy activity [*Bryden and Heath*, 1985].

Water column stability often has been invoked as an important factor influencing production in Antarctic waters [e.g., *Jacques*, 1989; *Nelson and Smith*; 1991] in that turbulent mixing controls irradiance and nutrient availability. South of the PF and north of the STF the Brunt-Väisälä frequency (Figure 5) indicates that the depths of relatively strong stratification were shallower than the euphotic zone (Table 2); thus phytoplankton should remain at depths where there was sufficient light to drive photosynthesis [*Sakshaug and Holm-Hansen*, 1986]. Between the PF and the SAF, however, deeper mixing may occur.

Near the PF the strongest and shallowest (40–50 m) stratification was on the upstream section, P14S (Figure 5), which would appear to be a favorable environment for phytoplankton. Despite this the highest chlorophyll (> 0.7 μg L^{-1}) and POC (8–10 μ*M*) concentrations occurred between the two branches of the PF in an area of relatively weak stratification (Figure 5) and slow current velocity (Figure 4). This biomass accumulation extended down to ~100 m where the buoyancy frequency was higher. In contrast, on the downstream section P15S the maximum chlorophyll (> 1 μg L^{-1}) and POC (>25 μ*M*) concentrations occurred south of the PF where stratification was relatively shallow (~50 m, Figure 5) and the current velocity was lower (16 cm s^{-1}) than on the upstream section (Figure 4). Although the pycnocline (Figure 3) was closer to the surface and stronger on P14S, current velocities were stronger (27 cm s^{-1}) on P14S than downstream on P15S, possibly related to the fact that the Pacific-Antarctic Ridge was steeper and oriented NW-SE below P14S and broader and oriented SW-NE below P15S. POC accumulation also was coincident with low current velocity in the northern regions of the sections. The highest POC concentration (14 μ*M*) on P14S occurred just north of the SAF, and POC > 15 μ*M* were found between the two branches of the STF on P15S.

Because phytoplankton growth is relatively low (0.2–0.3 doublings per day) (K. Daly and W. Smith, unpublished data, 1996), it is unlikely that high biomass accumulations can occur even downstream because of vertical motion [1–100 m d^{-1}) [*Veth et al.*, 1997] and horizontal advective loss in regions of high zonal velocities. Rather, accumulation may occur only in areas between the fronts where velocities are diminished (2-5 cm s^{-1}) or in meanders and eddies [e.g., *Heywood and Priddle*, 1987]. Although our data are limited, a biomass accumulation in the vicinity of the eddy at station 9 north of the SAF is suggested by an increase in POC and a deep chlorophyll maximum.

It is unlikely that nitrogen or phosphorus limited phytoplankton growth. Near-surface nitrate (12–27 μ*M*, Figures 6a and 6b) and phosphate concentrations (~1.0-2.1 μ*M*, Figures 7a and 7b) remained high throughout the region south of the STF. In addition, ammonium and urea, which may be preferentially taken up by Antarctic phytoplankton [*Probyn and Painting*, 1985], provided an additional source of nitrogen during our study. Ammonium concentrations observed in this study are within the range of those reported for the Atlantic [*Whitehouse et al.*, 1996; *Quéguiner et al.,* 1997] and Indian Ocean sectors [*Bianchi et al.*, 1997].

In contrast, silica and/or iron (Fe) limitation appear to be important factors governing phytoplankton growth and community composition. During our study, there was a marked gradient in silicic acid concentrations, with high (20-70 μ*M*) concentrations south of the PF (Figures 7c and 7d) and a rapid decrease (from > 20 to < 2 μ*M*) over ~200 km near the southern branch of the PF on P15S. This "silica front" is a major biogeochemical feature of the region and represents a rapid transition from a region where excess silicic acid occurs (and hence no silica limitation) to one where silica is most likely limiting to diatom growth [*Franck et al.,* 2000]. Si half-saturation constants K_s typically range from 0.5 to 5.0 μ*M* for different species of diatoms [*Nelson and Tréguer*, 1992], but some Antarctic diatoms have considerably higher K_s values (~8–89 μ*M*) [*Jacques*, 1983; *Sommer*, 1991] and would be Si-limited over much of the study area. Indeed, diatoms, such as *Nitzschia cylindrus*, *Chaetoceros* spp., and *Fragilariopsis sp.*, were the dominant biomass component at stations 35–48 (K. Buck, personal communication, 1997). North of these stations (~59°S), where Si concentrations were low, phytoplankton assemblages were dominated by small flagellates and microheterotrophs, which did not require Si. There also is a growing body of evidence indicating that dissolved Fe concentrations are very low in surface waters of the ACC and that Fe limitation or colimitation of Fe and Si occur [*de Baar et al.*, 1995; *Sedwick et al.*, 1997; *Timmermans et al.*, 1998; *Boyd et al.*, 1999, 2000].

4.4. Processes Influencing Si-Depleted Waters

The distribution pattern of excess nitrate and low silicic acid concentrations is similar throughout circumpolar waters between the PF and the STF [*Zentara and Kamykowski,* 1981; *Gordon and Molinelli*, 1982]. However, the processes generating the low silicic acid waters observed north of the PF have not been known. Because these patterns were observed during summer, it was assumed that the low Si concentrations were a result of uptake by diatoms, which use Si to form valves. One potential mechanism is that diatoms under Fe-limited conditions continue to incorporate silica relative to nitrogen, which results in particulate matter with elevated Si/N ratios [*Hutchins and Bruland,* 1998; *Takeda,* 1998]. In Pacific waters south of the Si gradient, under Fe-limited conditions, $Si(OH)_4$:NO_3^- uptake ratios as high as 8 were measured [*Franck et al.*, 2000], which clearly would result in rapid Si utilization. Low dissolved Fe levels may be common throughout the ACC [*Sedwick et al.*, 1997; *Boyd et al.,* 1999], except in regions where Fe-rich water is upwelled or downstream from islands and continents [*de Baar et al.*, 1995; *Sullivan et al.*, 1993]. Our study area was too distant from any land mass to benefit from this affect.

Another mechanism leading to low Si concentrations is differential remineralization. Particulate and dissolved organic nitrogen primarily are recycled within the surface layer by heterotrophic processes, whereas biogenic silica largely sinks to greater depths before being remineralized. Remineralization rates decrease in colder water, further contributing to the surface deficit in polar waters. This differential remineralization may lead to a decoupling of Si and N (i.e., a "silica pump"), resulting in extremely low dissolved Si/N ratios [*Dugdale et al.,* 1995].

Low silicic acid concentrations may limit diatom (and silicoflagellate and radiolarian) growth and thus influence community composition but does not limit productivity of the remaining phytoplankton assemblage. Nevertheless, this limitation has important consequences for the biological pump since diatom sedimentation is a central process for C and Si export into deep water [*Buessler*, 1998]. Although the mechanisms described above operate during the productive season, a more significant point is that there is no large source of silicic acid in the waters below the mixed layer to replenish surface waters during winter mixing or from downstream advection from the Indian Ocean sector.

On the basis of scant data, mixed layer depths during winter are 100-250 m in the Polar Frontal Zone and up to 400-600 m in the Subantarctic Frontal Zone [*McCartney*, 1977; *Gordon and Molinelli*, 1982; *Rintoul and Bullister*, 1999], although mixing to < 100 m may be common in both regions [reviewed by *Banse* [1996]). Nitrate concentrations at 200 m range from 15 to 25 μM and therefore winter replenishment of nitrate to these levels is likely. Silicic acid concentrations, however, are between 4 and 10 μM at 100–250 m below the Polar Frontal Zone and ~4 μM at those depths in the Subantarctic Zone. At 50° S the 10 μM Si isopleth is at ~700 m. This range of concentrations (4–10 μM) is consistent with surface values observed in early spring in the subantarctic region south of New Zealand [*Chang and Gall*, 1998; *Boyd et al.*, 1999] and in winter at an upstream site south of Australia [*Rintoul and Bullister*, 1999]. The seasonal change in mixed layer Si levels then would be ~2–8 μM. Removal by biological processes of this rather limited amount of silica, especially under Fe limitation and the resulting altered uptake ratios, could then occur over the timescales of weeks to months, resulting in the observed Si-depleted surface layer.

Other physical processes also may replenish nutrients in the surface layer during summer and influence regional production. Isopycnal displacements at eddies and fronts may bring water with higher nutrient concentrations into the euphotic zone. One cold-core eddy south of New Zealand in Subantarctic waters extended to 2000 m with isotherms that shoaled upward ~350 m [*Piola and Georgi*, 1982]. Vertical velocities in fronts and eddies range from 1 to 100 m d^{-1} (reviewed by *Veth et al.* [1997]). Such vertical transport within the numerous fronts and eddies in the region would be one means by which macronutrients and micronutrients might be injected into the surface layer. In our study, calculated geostrophic velocities ranged above 27 cm s^{-1} in the PF and 50 cm s^{-1} in the SAF (Figure 4), typical of frontal velocities in the ACC [*Hofmann*, 1985; *Abbott et al.,* 2000]. The resulting strong shears provide energy for significant eddy activity in the region [*Wunsch and Stammer*, 1995]. Eddies formed at the PF also may carry Si- and Fe-rich water into the Polar Frontal Zone. Hence either horizontal or vertical fluxes or both may be important in sustaining additional production during summer.

4.5. Carbon Export

The low abundance of relatively small-sized diatoms in surface samples between the PF and the STF during our study (K. Buck, personal communication, 1997) indicates that the vertical supply of Si to the surface layer during summer may be small and that diatom population growth may be balanced by grazing and sinking/advection. Small diatoms are less likely to sink from the surface layer than the large, heavily silicified ones found south of the PF. This hypothesis is supported by the results of another study in the same region. *Honjo et al.* [2000] observed that the carbon flux at 1000 m in the Subantarctic Zone was relatively low (1 g C m^{-2} yr^{-1}) and that the settling material was primarily calcium carbonate from coccoliths. In the vicinity of the PF and farther south, however, these investigators reported that carbon fluxes are twofold higher than the ocean average (1.7–2.3 g C m^{-2} yr^{-1}) and the material was dominantly biogenic silica from sinking diatoms. This finding is corroborated by the large opal deposits found in sediments south of the PF [*Kumar et al.*, 1995; *Tréguer et al.,* 1997].

Martin [1990] suggested that the Southern Ocean was a greater sink for atmospheric CO_2 during the Last Glacial Maximum due to an increase in Fe-rich aeolian dust to surface waters and subsequent increase in marine primary productivity. The flux of dust to the Antarctic continent was estimated to be twentyfold higher during the last glacial period [*Petit et al.*, 1981], and the Fe flux to sediments was estimated to be fivefold higher [*Kumar et al.*, 1995]. Whereas modern sediments in the Subantarctic Zone are dominantly carbonate with relatively low C, sediment cores suggest that export of C and opal increased during glacial periods because of increased Fe-dust deposition [*Kumar et al.*, 1995]. The accumulation of C and opal in glacial sediments, however, was uncoupled with greater C accumulation farther north in the subantarctic. A meandering PF, cooling surface water, and increased Fe could have permitted Antarctic diatom species to prosper farther north [*Moore et al.*, 2000]. The decline in opal at more north-

erly sites suggests that Si may have limited the growth of large diatoms even under Fe-replete conditions, and growth of small diatoms may have been balanced by grazing. Small diatoms also are less likely to sink from the surface layer, but they could be transported to intermediate depths through water mass formation processes, including subduction and diapycnal mixing.

Total organic carbon (TOC) is another source of carbon for export. TOC concentrations observed in the surface layer (50–80 μM) during our study were somewhat higher than those reported for the Ross Sea (40-60 μM [*Carlson et al.*, 1998]), similar to those reported from the central equatorial Pacific and Indian Oceans [*Carlson and Ducklow*, 1995; *Dovel and Hansell*, 2000], and lower than those reported for northern high latitudes (> 100 μM [*Anderson et al.*, 1994; *Daly et al.*, 1999]). TOC concentrations in the surface layer may have increased by ~17 μM during summer [*Dovel and Hansell*, 2000], a seasonal accumulation similar to that reported for other regions [e.g., *Carlson et al.*, 1994; *Daly et al.*, 1999].

Biological processes appeared to be an important factor controlling the distribution of TOC. The contribution of particulate organic carbon to the total organic carbon pool was small during our study, averaging ~12%, with a maximum of 30%, and no horizontal gradients in this ratio were detected. In waters on the Ross Sea continental shelf, *Carlson et al.* [1998] found that a large majority of the phytoplankton production was partitioned into particulate matter and only a small fraction was added to the DOC pool. If temperature were the dominant factor controlling carbon partitioning, we would have expected to see a latitudinal trend of increasing DOC/TOC ratios within our transects; however, none was observed. This suggests that the extent of biological processing of particulate matter by the localized food web may be the dominant factor regulating the production of semilabile and refractory DOC [*Legendre and Le Fevre,* 1995].

Physical processes also influenced the distribution of TOC. South of the PF, there appeared to be little vertical export of TOC by turbulent mixing during our study. North of the PF, however, TOC was transported to depth in subducted surface water, accounting for ~33% of the oxygen consumption in the upper 500 m [*Doval and Hansell*, 2000]. Dissolved inorganic carbon and small organic and inorganic particles also may be removed from the surface layer in this manner. Below 500 m, labile organic matter did not appear to be as important in AAIW as was observed in the Indian Ocean sector [*Moriarty et al.*, 1997]. Using an inverse box model, *Sloyan and Rintoul* [2001] estimated a diapycnal flux of 8 x 10^6 m^3 s^{-1} between Antarctic Surface Water and AAIW in the Pacific sector and 34 x 10^6 m^3 s^{-1} throughout the ACC. This downward transport to intermediate depths is similar to the upwelling flux of water (~20–40 x 10^6 m^3 s^{-1} [*Watson et al.*, 2000]), but about a factor of 4 greater than estimates of deepwater formation in the Southern Ocean (8–9.5 x 10^6 m^3 s^{-1} [*Orsi et al.*, 1999]). Hence subduction and diapycnal flux may be important processes contributing to carbon export from the surface layer.

4.6. Summary

Our results emphasize the physical, chemical, and biological complexity of the Antarctic Circumpolar Current. In this region of the Southern Ocean, physical processes generate a chemical gradient that provides a changing environment for phytoplankton growth. That is, the various fronts, jets, and convergence zones give rise to a nutrient field that permits diatom blooms and subsequent flux in Si-rich waters near the PF but Si limitation of diatom growth in the waters north of the Polar Front. This in turn has profound impacts on biological properties, such as community structure and flux of carbon, in each area. An increase in aeolian Fe to the immense area covered by the Polar and Subantarctic Zones may increase primary productivity overall and potentially increase the drawdown of atmospheric CO_2. Diatom growth, however, would still be limited by Si, and carbon export to deep water may remain relatively low.

South of the PF, particulate flux from sinking diatoms appears to be the primary mechanism for carbon export to deep water based on sediment trap results [*Honjo et al.*, 2000] and the large accumulation of siliceous deposits in this region of the ACC [*Kumar et al.*, 1995; *Tréguer et al.,* 1997]. North of the PF, however, our results suggest that both particulate and dissolved carbon may be exported from the surface layer to intermediate depths (SAMW and AAIW) primarily through water mass formation processes, including subduction and diapycnal mixing.

The Southern Ocean and, in particular, the frontal regimes between 50° and 60°S are critical to understanding not only the global carbon cycle [*Sarmiento and LeQuéré,* 1996] but also the global silica cycle [*Tréguer et al.,* 1997]. In addition, this region may be sensitive to global change [*Sarmiento and LeQuéré,* 1996], and it appears to have had a large but poorly defined role in paleoclimates [e.g., *Kumar et al.*, 1995; *Moore et al.*, 2000]. Given the region's extreme importance, further investigation of integrated physical-biological processes that influence the distributions of nutrients, carbon, and biogenic matter appears warranted. In particular, the role of physical processes that control the Si supply to surface waters and C removal to intermediate or greater depths should be evaluated by models to improve predictions about changes in the ocean's C cycle due to climate forcing.

Acknowledgments. We thank the crew of the NOAA Ship *Discoverer* for assistance during the cruise and S. Polk, A.-M. White, and L. Cooper for technical assistance. TCO_2 measurements were provided by M. Roberts and fCO_2 measurements were provided by R. Wanninkhof. F. Chavez kindly provided unpublished data that contributed to the interpretation of results. We are also grateful to A. Dickson and an anonymous reviewer for their editorial comments. This research was supported by the NOAA/ OGP Ocean-Atmosphere Carbon Exchange Study. K.L. Daly also was supported by an Alexander Hollaender Distinguished Postdoctoral Fellowship sponsored by the United States Department of Energy and administered by the Oak Ridge Institute for Science and Education, and G.C. Johnson had additional support from the NASA Physical Oceanography Program. C.W. Mordy was supported by the Joint Institute for the Study of the Atmosphere and Ocean (JISAO) under NOAA Cooperative Agreement NA67RJO155, contribution 739.

References

Abbott, M.R., J.G. Richman, R.M. Letelier, and J.S. Bartlett, The spring bloom in the Antarctic Polar Frontal Zone as observed from a mesoscale array of bio-optical sensors, *Deep Sea Res., Part II, 47*, 3285-3314, 2000.

Anderson, L.G., K. Olsson, and A. Skoog, Distribution of dissolved inorganic and organic carbon in the Eurasian Basin of the Arctic Ocean, in *The Polar Oceans and Their Role in Shaping the Global Environment, Geophys. Monogr. Ser.*, vol. 85, edited by O.M. Johannessen, R.D. Muench, and J.E. Overland, pp. 255-262, AGU, Washington, D.C., 1994.

Bakker, D.C.E., H.J.W. de Baar, and U.V. Bathmann, Changes of carbon dioxide in surface waters during spring in the Southern Ocean, *Deep Sea Res. Part II*, *44*, 91-127, 1997.

Banse, K., Low seasonality of low concentrations of surface chlorophyll in the Subantarctic water ring: Underwater irradiance, iron, or grazing?, *Prog. Oceanogr., 37*, 241-291, 1996.

Banse, K., and D.C. English, Near-surface phytoplankton pigment from the Coastal Zone Color Scanner in the Subantarctic region southeast of New Zealand, *Mar. Ecol. Prog. Ser.*, *156*, 51-66, 1997.

Bianchi, M., F. Feliatra, P. Treguer, M.-A. Vincendeau, and J. Morvan, Nitrification rates, ammonium and nitrate distributions in upper layers of the water column and in sediments of the Indian sector of the Southern Ocean, *Deep Sea Res. Part II*, *44*, 1017-1032, 1997.

Boyd, P., J. LaRoche, M. Gall, R. Frew, and R.M.L. McKay, Role of iron, light, and silicate in controlling algal biomass in subantarctic waters SE of New Zealand, *J. Geophys. Res.*, *104*, 13,395-13,408, 1999.

Boyd, P.W., et al., A mesoscale phytoplankton bloom in the polar Southern Ocean stimulated by iron fertilization, *Nature*, *407*, 695-702, 2000.

Bradford-Grieve, J.M., P.W. Boyd, F.H. Chang, S. Chiswell, M. Hadfield, J.A. Hall, M.R. James, S.D. Nodder, and E.A. Shushkina, Pelagic ecosystem structure and functioning in the Subtropical Front region east of New Zealand in austral winter and spring 1993, *J. Plankton Res.*, *21*, 405-428, 1999.

Bryden, H.L. ,and R.A. Heath, Energetic eddies at the northern edge of the Antarctic Circumpolar Current in the Southwest Pacific, *Prog. Oceanogr., 14*, 65-87, 1985.

Buessler, K.O., The decoupling of production and particulate export in the surface ocean, *Global Biogeochem. Cycles*, *12*, 297-310, 1998.

Carlson, C.A., and H.W. Ducklow, Dissolved organic carbon in the upper ocean of the central equatorial Pacific Ocean, 1992: Daily and fine-scale vertical variations, *Deep Sea Res., Part II*, *42*, 639-656, 1995.

Carlson, C.A., H.W. Ducklow, and A.F. Michaels, Annual flux of dissolved organic carbon from the euphotic zone in the northwestern Sargasso Sea, *Nature*, *371*, 405-408, 1994.

Carlson, C.A., H.W. Ducklow, D.A. Hansell, and W.O. Smith Jr., Organic carbon partitioning during spring phytoplankton blooms in the Ross Sea polynya and the Sargasso Sea, *Limnol. Oceanogr., 43,* 375-386, 1998.

Chang, F.H., and M. Gall, Phytoplankton assemblages and photosynthetic pigments during winter and spring in the subtropical convergence region near New Zealand, *N. Z. J. Mar. Freshwater Res., 32*, 515-530, 1998.

Chen, C.-T.A., On the distribution of anthropogenic CO_2 in the Atlantic and Southern oceans, *Deep Sea Res., Part A*, *29*, 563-580, 1982.

Clementson, L.A., J.S. Parslow, F.B. Griffiths, V.D. Lyne, D.J. Mackey, G.P. Harris, D.C. McKenzie, P.I. Bonham, C.A. Rathbone, and S. Rintoul, Controls on phytoplankton production in the Australasian sector of the subtropical convergence, *Deep Sea Res., Part I*, *45*, 1627-1661, 1998.

Comiso, J.C., C.R. McClain, C.W. Sullivan, J.P. Ryan, and C.L. Leonard, Coastal Zone Color Scanner pigment concentrations in the Southern Ocean and relationships to geophysical surface features, *J. Geophys. Res.*, *98*, 2419-2451. 1993.

Daly, K.L., D.W.R. Wallace, W.O. Smith Jr., A. Skoog, R. Lara, M. Gosselin, E. Falck, and P. Yager, Non-Redfield carbon and nitrogen cycling in the Arctic: Effects of ecosystem structure and dynamics, *J. Geophys. Res.*, *104*, 3185-3199, 1999.

de Baar, H.J.W., J.T.M. de Jong, D.C.E. Bakker, B.M. Löscher, C. Veth, U. Bathmann, and V. Smetacek, Importance of iron for phytoplankton blooms and carbon dioxide drawdown in the Southern Ocean, *Nature*, *373*, 412-415, 1995.

Doval, M.D., and D. A. Hansell, Organic carbon and apparent oxygen utilization in the western South Pacific and the central Indian Oceans, *Mar. Chem.*, *68*, 249-264, 2000.

Dugdale, R.C., F.P. Wilkerson, and H.J. Minas, The role of a silicate pump in driving new production, *Deep Sea Res., Part I*, *42*, 697-719, 1995.

El-Sayed, S.Z., Phytoplankton production of the South Pacific and the Pacific sector of the Antarctic, in *Scientific Exploration of the South Pacific*, pp. 194-210, Natl. Acad. Sci., Washington, D. C., 1970.

Fine, R.A., Circulation of Antarctic Intermediate Water in the South Indian Ocean, *Deep Sea. Res., Part I*, *40*, 2021-2042, 1993.

Franck, V.M., M.A. Brzezinski, K.H. Coale, and D.M. Nelson, Iron and silicic acid concentrations regulate Si uptake north and south of the Polar Frontal Zone in the Pacific Sector of the Southern Ocean, *Deep Sea Res., Part II*, *47*, 3315-3338, 2000.

Fukuchi, M., Phytoplankton chlorophyll stocks in the Antarctic Ocean, *J. Oceanogr. Soc. Jpn.*, *36*, 73-84, 1980.

Garner, D.M., The Sub-tropical Convergence in New Zealand surface waters, *N.Z.J. Geol. Geophys.*, *2*, 315-337, 1959.

Gille, S.T., Mean surface height of the Antarctic Circumpolar Current from Geosat data: Method and application, *J. Geophys. Res.*, *99*, 18,255-18,273, 1994.

Gille, S.T., and K.A. Kelly, Scales of spatial and temporal variability in the Southern Ocean, *J. Geophys. Res.*, *101*, 8759-8773, 1996.

Gordon, A.L., and E. Molinelli, *Southern Ocean Atlas*, Columbia Univ. Press, New York, 11 pp., 233 plates, 1982.

Gordon, L.I., J.C. Jennings Jr., A.A. Ross, and J.M. Krest, A suggested protocol for continuous flow automated analysis of seawater nutrients (phosphate, nitrate, nitrite and silicic acid) in the WOCE Hydrographic Program and the Joint Global Ocean Fluxes Study, in *WOCE Operations Manual*, 3.1.3, WHP Operations and Methods Manual 91-1, 1993.

Hansell, D.A., and C.A. Carlson, Deep-ocean gradients in the concentration of dissolved organic carbon, *Nature, 395,* 283-285, 1998.

Heath, R.A., Large-scale influence of the New Zealand seafloor topography on western boundary currents of the South Pacific Ocean, Australia, *J. Mar. Freshwater Res., 36,* 1-14, 1985.

Heywood, R.B., and J. Priddle, Retention of phytoplankton by an eddy, *Cont. Shelf Res., 7*, 937-955, 1987.

Hofmann, E.E., The large-scale horizontal structure of the Antarctic Circumpolar Current from FGGE drifters, *J. Geophys. Res.*, *90*, 7087-7097, 1985.

Holm-Hansen, O., S.Z. El-Sayed, G.A. Fraceschini, and R.L. Cuhel, Primary production and the factors controlling phytoplankton growth in the Southern Ocean, in *Adaptations Within Antarctic Ecosystems*, edited by G. Llano, pp. 11-50, Gulf Publ., Houston, Tex., 1977.

Honjo, S., R. Francois, S. Manganini, J. Dymond, and R. Collier, Particle fluxes to the interior of the Southern Ocean in the western Pacific sector along 170°W, *Deep Sea Res., Part II, 47*, 3521-3548, 2000.

Hoppema, M., E. Fahrbach, M. Schroeder, A. Wisotzki, and H.J.W. De Baar, Winter-summer differences of carbon dioxide and oxygen in the Weddell Sea surface layer, *Mar. Chem., 51*, 177-192, 1995.

Hutchins, D.A., and K.W. Bruland, Iron-limited diatom growth and Si:N uptake ratios in a coastal upwelling regime, *Nature*, *393*, 561-564, 1998.

Jacques, G., Some ecophysiological aspects of Antarctic phytoplankton, *Polar. Biol.*, *2*, 27-33, 1983.

Jacques, G., Primary production in the open Antarctic Ocean during the austral summer: A review, *Vie Milieux*, *39*, 1-17, 1989.

Kumar, N., R.F. Anderson, R.A. Mortlock, P.N. Froelich, O. Kubik, B. Dittrich-Hannen, and M. Suter, Increased biological productivity and export production in the glacial Southern Ocean, *Nature*, *378*, 675-680, 1995.

Lamb, M.F., et al., Chemical and hydrographic measurements in the eastern Pacific during the CGC94 expedition (WOCE section P18), *NOAA Data Rep. ERL PMEL-61a (PB97-158075)*, 235 pp., Natl. Oceanic and Atmos. Admin., Silver Springs, Md., 1997.

Legendre, L., and J. Le Fevre, Microbial food webs and the export of biogenic carbon in oceans, *Aquat. Microbiol. Ecol., 9,* 69-77, 1995.

Longhurst, A.R., Role of the marine biosphere in the global carbon cycle, *Limnol. Oceanogr.*, *36*, 1507-1526, 1991.

Martin, J.H., Glacial-interglacial CO_2 change: The iron hypothesis, *Paleoceanography*, *5*, 1-13, 1990.

McCartney, M.S., Subantarctic mode water, in *Voyage of Discovery*, edited by M. Angel, pp. 103-119, Pergamon, New York, 1977.

McCartney, M.S., The subtropical recirculation of mode waters, *J. Mar. Res.*, *40*, 427-464, 1982.

McTaggart, K.E., and G.C. Johnson, CTD/O_2 Measurements col-

lected on a Climate and Global Change Cruise (WOCE Sections P14S and P15S) during January-March, 1996, *NOAA Data Rep. ERL PMEL-63*, 485 pp., Natl. Oceanic and Atmos. Admin., Silver Spring, Md., 1997.

Metzl, N., C. Beauverger, C. Brunet, C. Goyet, and A. Poisson, Surface water carbon dioxide in the southwest Indian sector of the Southern Ocean: A highly variable CO_2 source/sink region in summer, *Mar. Chem.*, *35*, 85-95, 1991.

Minas, H.J., and M. Minas, Net community production in "high nutrient-low chlorophyll" waters of the tropical and Antarctic Oceans: Grazing vs iron hypothesis, *Oceanol. Acta*, *15*, 145-162, 1992.

Molinelli, E., The Antarctic influence on Antarctic Intermediate Water, *J. Mar. Res.*, *39*, 267-293, 1981.

Moore, J.K., M.R. Abbott, and J.G. Richman, Location and dynamics of the Antarctic Polar Front from satellite sea surface temperature data, *J. Geophys. Res., 104,* 3059-3073, 1999a.

Moore, J.K., M.R. Abbott, J.G. Richman, W.O. Smith, T.J. Cowles, K.H. Coale, W.D. Gardner, and R.T. Barber, SeaWiFS satellite ocean color data at the U.S. Southern Ocean JGOFS line along 170°W, *Geophys. Res. Lett., 26*, 1465-1468, 1999b.

Moore, J.K., M.R. Abbott, J.G. Richman, and D.M. Nelson, The Southern Ocean at the Last Glacial Maximum: A strong sink for atmospheric carbon dioxide, *Global Biogeochem. Cycles*, *14*, 455-475, 2000.

Moriarty, D.J.W., M. Bianchi, and V. Talbot, Bacterial productivity and organic matter flux in the Southern Ocean and in the Antarctic Intermediate Water and mode water of the Indian Ocean, *Deep Sea Res., Part II*, *44*, 1005-1015, 1997.

Morrow, R., J. Church, R. Coleman, D. Chelton, and N. White, Eddy momentum flux and its contribution to the Southern Ocean momentum balance, *Nature*, 357, 482-484, 1992.

Mulvenna, P.F., and G. Savidge, A modified manual method for the determination of urea in seawater using diacetylmonoxime reagent, *Estuarine Coastal Shelf Sci.*, *34*, 429-438, 1992.

Murphy, P.P., R.A. Feely, R.H. Gammon, D.E. Harrison, K.C. Kelly, and L.S. Waterman, Assessment of the air-sea exchange of CO_2 in the south Pacific during austral autumn, *J. Geophys. Res., 96*, 20,455-20,465, 1991.

Nelson, D.M., and W.O. Smith Jr., Sverdrup revisited: Critical depths, maximum chlorophyll levels, and the control of Southern Ocean productivity by the irradiance-mixing regime, *Limnol. Oceanogr.*, *36*, 1650-1661, 1991.

Nelson, D.M., and P. Tréguer, Role of silicon as a limiting nutrient to Antarctic diatoms: Evidence from kinetic studies in the Ross Sea ice-edge zone, *Mar. Ecol. Prog. Ser.*, *80*, 255-264, 1992.

Nowlin, W.D., and J.M. Klinck, The physics of the Antarctic Circumpolar Current, *Rev. Geophys., 24,* 469-491, 1986.

Orsi, A.H., T. Whitworth III, W.D. Nowlin Jr., On the meridional extent and fronts of the Antarctic Circumpolar Current, *Deep Sea Res., Part I, 42*, 641-673, 1995.

Orsi, A.H., G.C. Johnson, and J.L. Bullister, Circulation, mixing, and production of Antarctic Bottom Water, *Prog. Oceanogr.*, *43*, 55-109, 1999.

Parsons, T.R., Y. Maita, and C. Lalli, *A Manual of Chemical and Biological Methods for Seawater Analysis*, 173 pp., Pergamon, New York, 1984.

Petit, J.-R., M. Briat, and A. Royer, Ice age aerosol content from east Antarctic ice core samples and past wind strength, *Nature*, *293*, 391-394, 1981.

Piola, A.R., and D.T. Georgi, Circumpolar properties of Antarctic Intermediate Water and Subantarctic Mode Water, *Deep Sea Res.*, *29*, 687-711, 1982.

Probyn, T.A., and S.J. Painting, Nitrogen uptake by size-fractionated phytoplankton in Antarctic surface waters, *Limnol. Oceanogr.*, *30*, 1327-1332, 1985.

Quéguiner, B., P. Tréguer, I. Peeken, and R. Scharek, Biogeochemical dynamics and the silicon cycle in the Atlantic sector of the Southern Ocean during austral spring 1992, *Deep Sea Res., Part II, 44,* 69-90, 1997.

Reed, J.F., and R.T. Pollard, Structure and transport of the Antarctic Circumpolar Current and Agulhas return current at 40° E, *J. Geophys. Res.*, *98*, 12,281-12,295, 1993.

Rintoul, S.R., and J.L. Bullister, A late winter hydrographic section from Tasmania to Antarctica, *Deep Sea Res., Part I, 46*, 1417-1454, 1999.

Rintoul, S.R., J.R. Donguy, and D.H. Roemmich, Seasonal evolution of upper ocean thermal structure between Tasmania and Antarctica, *Deep Sea Res., Part 1, 44*, 1185-1202, 1997.

Robertson, J.E., and A.J. Watson, A summer-time sink for atmospheric carbon dixide in the Southern Ocean between 88°W and 80°E, *Deep Sea Res., Part II, 42*, 1081-1091, 1995.

Sabine, C.L., and R.M. Key, Controls on fCO_2 in the South Pacific, *Mar. Chem.*, *60*, 95-110, 1998.

Sakshaug, E., and O. Holm-Hansen, Photoadaptation in Antarctic phytoplankton: Variations in growth rate, chemical composition and *P* versus *I* curves, *J. Plankton Res.*, *8*, 459-473, 1986.

Sarmiento, J.L., and C. LeQuéré, Oceanic carbon dioxide uptake in a model of century-scale global warming, *Science, 274*, 1346-1350, 1996.

Sedwick, P.N., P.R. Edwards, D.J. Mackey, F.B. Griffiths, and J.S. Parslow, Iron and manganese in surface water of the Australian subantarctic region, *Deep Sea Res., Part I, 44*, 1239-1251, 1997.

Sloyan, B.M., and S.R. Rintoul, Circulation, renewal and modification of Antarctic Mode and Intermediate Water, *J. Phys. Oceanogr.*, in press, 2001.

Smetacek, V., H.J.W. de Baar, U.V. Bathmann, K. Lochte, and M.M.R. van der Loeff, Ecology and biogeochemistry of the Antarctic Circumpolar Current during austral spring: A summary of the Southern Ocean JGOFS cruise ANT X/6 of R.V. *Polarstern, Deep Sea Res., Part II, 44*, 1-21, 1997.

Sommer, U., Comparative nutrient status and competitive interactions of two Antarctic diatoms (*Corethron criophilum* and *Thalassiosira antarctica*), *J. Pankton Res.*, *13*, 61-75, 1991.

Sullivan, C.W., K.R. Arrigo, C.R. McClain, J.C. Comiso, and J. Firestone, Distributions of phytoplankton blooms in the Southern Ocean, *Science*, *262*, 1832-1837, 1993.

Takahashi, T., R.A. Feely, R.F. Weiss, R.H. Wanninkhof, D.W. Chipman, S.C. Sutherland, and T.T. Takahashi, Global air-sea flux of CO_2: An estimate based on measurements of sea-air pCO_2 difference, *Proc. Natl. Acad. Sci. USA, 94*, 8292-8299, 1997.

Takeda, S., Influence of iron availability on nutrient consumption ratio of diatoms in oceanic waters, *Nature*, *393*,774-777, 1998.

Timmermans, K.R., M.A. van Leeuwe, J.T. de Jong, R.M.L. McKay, R.F. Nolting, H.J. Witte, J. van Ooyen, M.J.W. Swagerman, H. Kloosterhuis, and H.J.W. de Baar, Iron stress in the Pacific region of the Southern Ocean: evidence from enrichment bioassays, *Mar. Ecol. Prog. Ser.*, *166*, 27-41, 1998.

Tréguer, P., D.M. Nelson, A. van Bennekom, D.J. DeMaster, A. Laynaert, and B. Quéguiner, The silica balance in the world ocean: A re-estimate, *Science*, *268*, 375-379, 1997.

UNESCO, The practical salinity scale 1978 and the international equation of state of seawater 1980, tenth report of the Joint Panel on Oceanographic Tables and Standards, *UNESCO Tech. Pap. Mar. Sci., 36*, 144 pp., 1981.

Veth, C., I. Peeken, and R. Scharek, Physical anatomy of fronts and surface waters in the ACC near the 6°W meridian during austral spring 1992, *Deep Sea Res., Part II, 44,* 23-50, 1997.

Wanninkhof, R., and K. Thoning, Measurement of fugacity of CO_2 in surface seawater using continuous and discrete sampling methods, *Mar. Chem.*, *44*, 189-204, 1993.

Watson, A.J., D.C.E. Bakker, A.J. Ridgwell, P.W. Boyd, and C.S. Law., Effect of iron on Southern Ocean CO_2 uptake and implications for glacial atmospheric CO_2, *Nature, 407*, 730-733, 2000.

Weiss, R.F., Carbon dioxide in water and seawater: The solubility of a non-ideal gas, *Mar. Chem.*, *2*, 203-215, 1974.

Whitehouse, M.J., J. Priddle, P.N. Trathan, and M.A. Brandon, Substantial open-ocean phytoplankton blooms to the north of South Georgia, South Atlantic, during summer 1994, *Mar. Ecol. Prog. Ser.*, *140*, 187-197, 1996.

Wijffels, S.E., J.M. Toole, H.L. Bryden, R.A. Fine, W.J. Jenkins, and J.L. Bullister, The water masses and circulation at 10°N in the Pacific, *Deep Sea Res., Part I, 43*, 501-544, 1996.

Wright, S.W., S.W. Jeffrey, R.F.C. Mantoura, C.A. Llewellyn, T. Bjørnland, D. Repeta, and N. Welschmeyer, Improved HPLC method for the analysis of chlorophylls and carotenoids from marine phytoplankton, *Mar. Ecol. Prog. Ser.*, *77*, 183-196, 1991.

Wunsch, C., and D. Stammer, The global frequency-wavenumber spectrum of oceanic variability estimated from TOPEX/Poseidon altimetry measurements, *J. Geophys. Res.*, *100*, 24,895-24,910, 1995.

Yamaguchi, Y., S. Kosaki, and Y. Aruga, Primary productivity in the

Antarctic Ocean during the austral summer of 1983/84, *Trans. Tokyo Univ. Fish.*, *6*, 67-84, 1985.

Zentara, S.-J., and D. Kamykowski, Geographic variations in the relationship between silicic acid and nitrate in the South Pacific Ocean, *Deep Sea Res., Part A, 28*, 455-465, 1981.

K. L. Daly, College of Marine Science, University of South Florida, 140 Seventh Ave. S., St. Petersburg, FL 33701 (e-mail: kdaly@marine.usf.edu).

W. O. Smith Jr., Virginia Institute of Marine Science, College of William and Mary, Glouster Pt., VA 23602.

R. A. Feely and G. C. Johnson, Pacific Marine Environmental Laboratory, NOAA, 7600 Sand Point Way NE, Seattle, WA 98115.

G. R. DiTullio, Grice Marine Lab, University of Charleston, 205 Fort Johnson, Charleston, SC 29412.

D. R. Jones, Haskin Shellfish Research Laboratory, Port Norris, NJ 08349.

C. W. Mordy, Joint Institute for the Study of Atmosphere and Ocean, University of Washington, Seattle, WA 98195.

D. A. Hansell, Rosenstiel School of Marine and Atmospheric Science, University of Miami, Miami, FL 33149.

J.-Z. Zang, Cooperative Institute for Marine and Atmospheric Studies, Rosenstiel School of Marine and Atmospheric Science, University of Miami, Miami, FL 33149.

(Received October 8, 1999; revised November 13, 2000; accepted December 14, 2000)